Tetrahedral Hohlraum High-Convergence Implosion Experiments on Omega ID4-FY98

August 31 – September 4, 1998

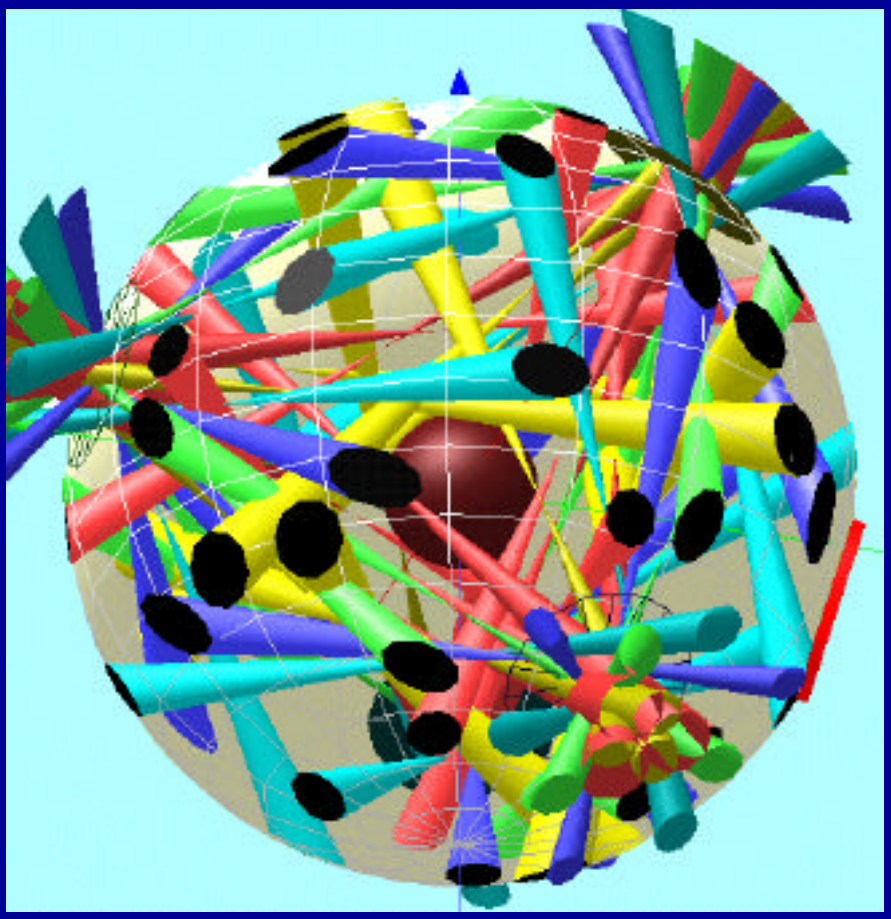

UR LLE

Los Alamos
Inertial Confinement Fusion

LA-UR-98-4056

LA-UR-98-4056

High-convergence implosions in tetrahedral hohlraums shot plan (ID4-FY98)

This document is intended to give an overview of this experimental campaign. Where information conflicts with experimental configurations submitted by official methods, those configurations take precedence. Contact the Principal Investigator prior to making any changes in the configuration to accommodate conflicts of information based on this document.

This document was produced by the Los Alamos National Laboratory under the auspices of the United States Department of Energy under contract no. W-7405-ENG-36.

Introduction and background

The utility of the Omega laser facility for indirect-drive inertial confinement fusion experiments has been irrefutably demonstrated [1-3]. Experiments have demonstrated that cylindrical hohlraums using up to 40 of the 60 Omega beams can be used to produce symmetric implosions with shapes predictable by existing ICF codes. [2]

Experiments have also been performed [4,5] that utilize spherical hohlraums with a tetrahedral arrangement of laser entrance holes [6,7], also known as "tetrahedral hohlraums." These experiments allow the use of all 60 Omega beams to drive implosions, and have potential symmetry advantages over cylindrical hohlraums. In the first set of experiments [8], x-ray drive and implosion symmetry and performance were measured using spherical hohlraums with 2300-μm inside diameter (scale-1) with 1 ns sq and shaped laser drives, and 2800-μm inside diameter (scale-1.2) with 1 ns sq laser drive. Implosion images obtained through a laser entrance (LEH) hole showed a distinctive m=3 component aligned with the LEHs.

A follow-up set of experiments utilized scale-1.2 hohlraums with reduced laser entrance hole diameters and shaped laser pulses. The combination created implosion images with almost no m=3 component in the shape. While fully-integrated three-dimensional calculations of the symmetry from an inherently three-dimensional experiment such as this are not available, simpler calculations indicate that these hohlraums produce a radiation drive with greatly reduced time-dependent asymmetry as compared to cylindrical hohlraums. Therefore, this configuration has the potential to allow implosion hydrodynamics experiments that do not have the complication of time-dependent drive asymmetry affecting the interpretation of the data.

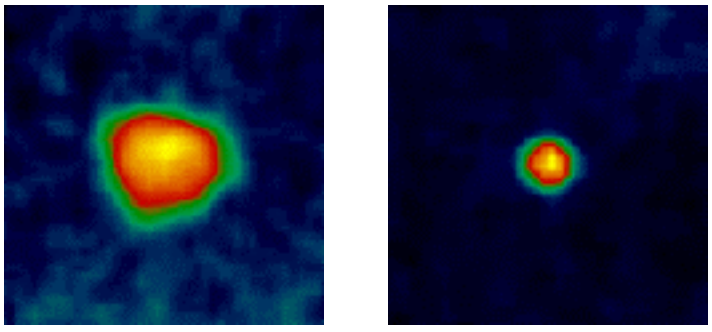

Figure 1: In the first set of tetrahedral experiments, implosion images contained a significant m=3 component (left), while larger hohlraums, smaller LEHs, and longer pulse shape reduced the m=3 component to negligible levels in a follow-up campaign (right).

Objectives

In this experiment, we will investigate the utility of tetrahedral hohlraums for:

- Driving capsules symmetrically in a time-dependent manner allowing investigations of capsule hydrodynamics without the complication of time-dependent symmetry effects;
- Driving planar packages for witness-plate radiation temperature measurements and for weapons physics experiments.

During this set of experiments, we will also activate two new Los Alamos diagnostics:

- Neutron bang time system capable of measuring the average time of neutron emission for targets yielding greater than ~10^8 DD neutrons to an accuracy of 100 ps;
- An optical telescope will be activated and demonstrated as a streaked optical pyrometer.

During the implosion experiment, two types of capsule will be utilized. “Standard” plastic capsules will be used in an experiment to measure the degradation of performance as convergence increases. Double shell capsules will be used to determine their potential as an alternate NIF ignition capsule design.

Experimental Plan

Target description

The targets will consist of thin-wall scale-1.2 spherical hohlraums (inside diameter of 2800 µm), with four 700-µm laser entrance holes arranged in a tetrahedral pattern. The wall will consist of 100 µm of epoxy (by weight, 74.4% C, 7.1% H, 18.1% O, 0.4% N; by atom, 42.8% C, 49.1% H, 18.1% O, 0.2% N; specific density =1.15) with a 2-µm gold lining.

The hohlraums will either contain a “double-shell” capsule or a high-convergence capsule with a nominal outside diameter of 550 µm, or will have a witness plate or experimental package on the side of the hohlraum for use with the streaked optical pyrometer being activated during this series. Targets with planar packages will also have shields to reduce scattered light and LEH views for the SOP.

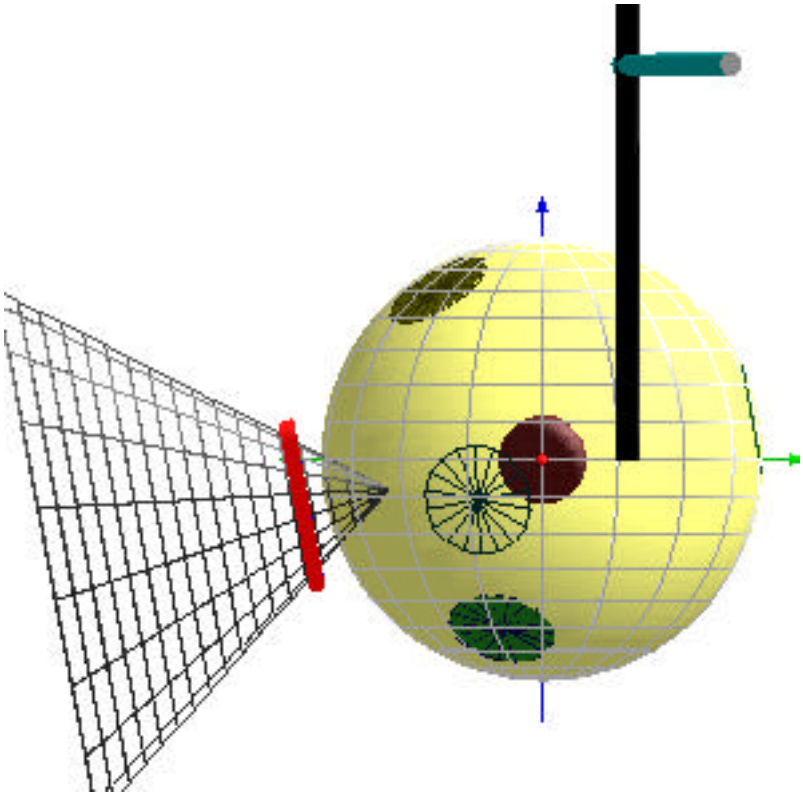

Figure 2: View of tetrahedral hohlraum from the North.

Alignment choice

On Omega, each of the hexagonal ports has six other hexagonal ports located 109.47° away, the angle for tetrahedral symmetry. These six consist of two groups of three ports which, in turn, are made up of ports 109.47° from each other. Each port, along with one of the groups of three, defines one tetrahedral alignment. Since there are 20 hexagonal ports, and each alignment uses four of the ports, there are ten unique tetrahedral alignments on Omega (Table 1). The choice of two ports 109.47° apart uniquely defines the alignment.

For the set of experiments performed in ID4-FY98, the 4-7 configuration will be used. This orientation was chosen due to the availability of certain diagnostics, the most important being TIM 5 which will hold the SOP and view the witness plates mounted opposite laser entrance hole B (LEH B), and TIM 2 which will hold XRFC4 to view the capsule through LEH B centered on H7. In addition, Dante will view the hohlraum wall through LEH D centered on H20 at a 42° angle, and LEH D will be monitored with XRFC3 with a soft-x-ray framing camera (SXRFC) snout from TIM 6.

Designation	Ports			
1-8	H1	H8	H14	H17
1-9	H1	H9	H11	H18
2-9	H2	H9	H13	H16
2-10	H2	H10	H15	H17
3-6	H3	H6	H14	H16
3-10	H3	H10	H12	H20
4-6	H4	H6	H11	H19
4-7	H4	H7	H13	H20
5-7	H5	H7	H15	H18
5-8	H5	H8	H12	H19

Table 2: Sets of hexagonal ports on Omega that constitute unique tetrahedrally symmetric orientations

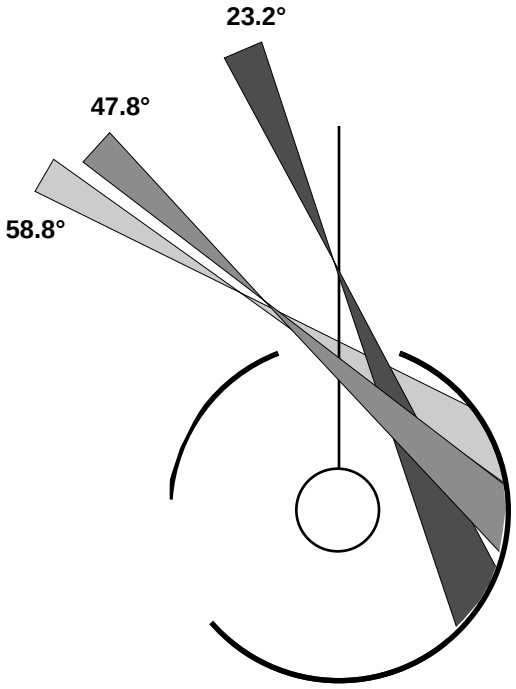

Figure 3: Illustration of the entrance angles of the beams in tetrahedral illumination of spherical Omega hohlraums.

Pointing scheme

The choice of beam pointing [9] is made based on having all 60 beams enter the hohlraum, not having the beams strike the capsule or one of the other laser entrance holes, and minimizing the flux asymmetries created due to the laser entrance holes. By necessity, the beams are pointed in such a way that they do not cross the axis of the laser entrance hole.

The beams can be divided into three cones according to their angle with respect to the ray from target chamber center through the laser entrance hole. In order of increasing angle, they are cone 1 (23.2°), cone 2 (47.8°), and cone 3 (58.8°). Cones 1 and 2 contain 6 beams each, and cone 3 contains 3 beams.

Beam cones 1 and 2 can be further divided into cones of 3 beams each according to whether or not they come close to laser entrance holes when they reach the far side of the hohlraum. Beam cones 1a and 2a come close, while cones 1b and 2b fall between laser entrance holes. Thus, pointing numbers can be derived for five different beam cones of 3 beam each per laser entrance hole.

(Note: this figure has been determined to be incorrect.)

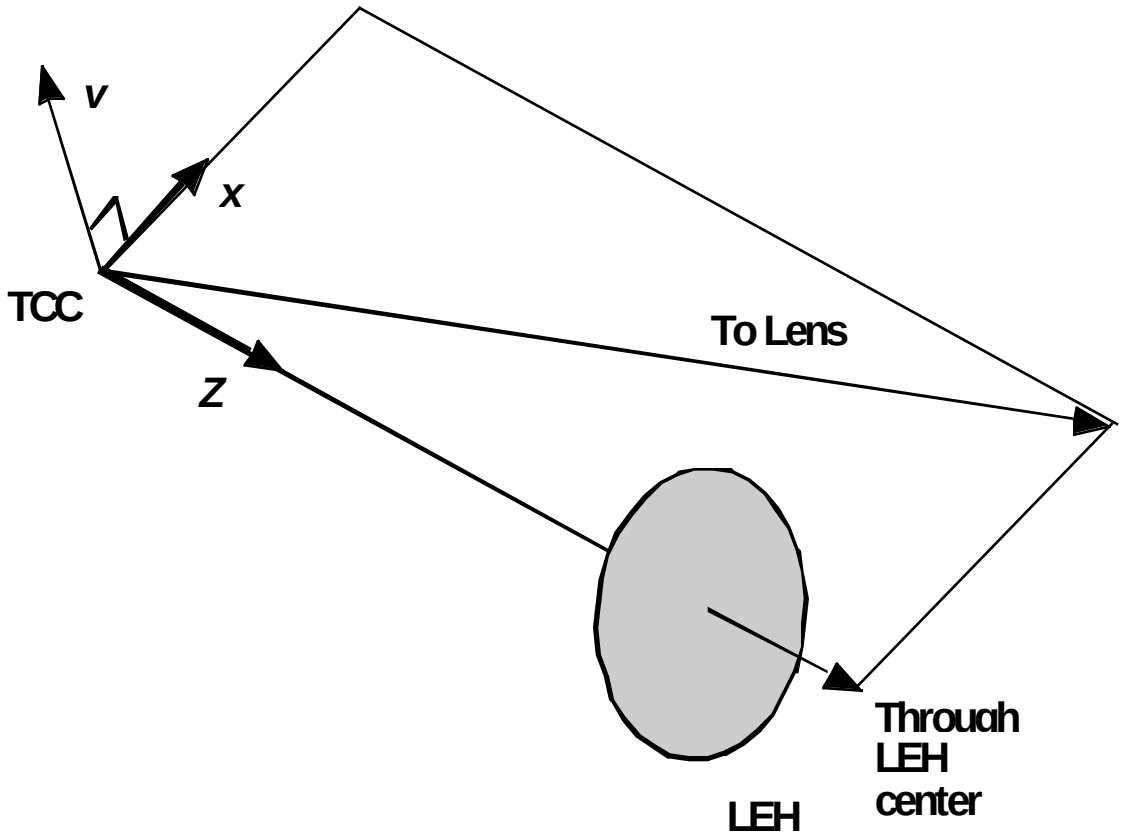

Figure 3: Coordinate system used in determining pointing for the beam cones in Omega tetrahedral hohlraums.

Beam Cone	X	Y	Z
1A	525	-45	256
1B	370	-50	700
2A	455	20	1035
2B	375	-170	1000
3	110	-50	1278

Table 2: Coordinates for the scale-1.2 tetrahedral pointing used in ID4-FY98.

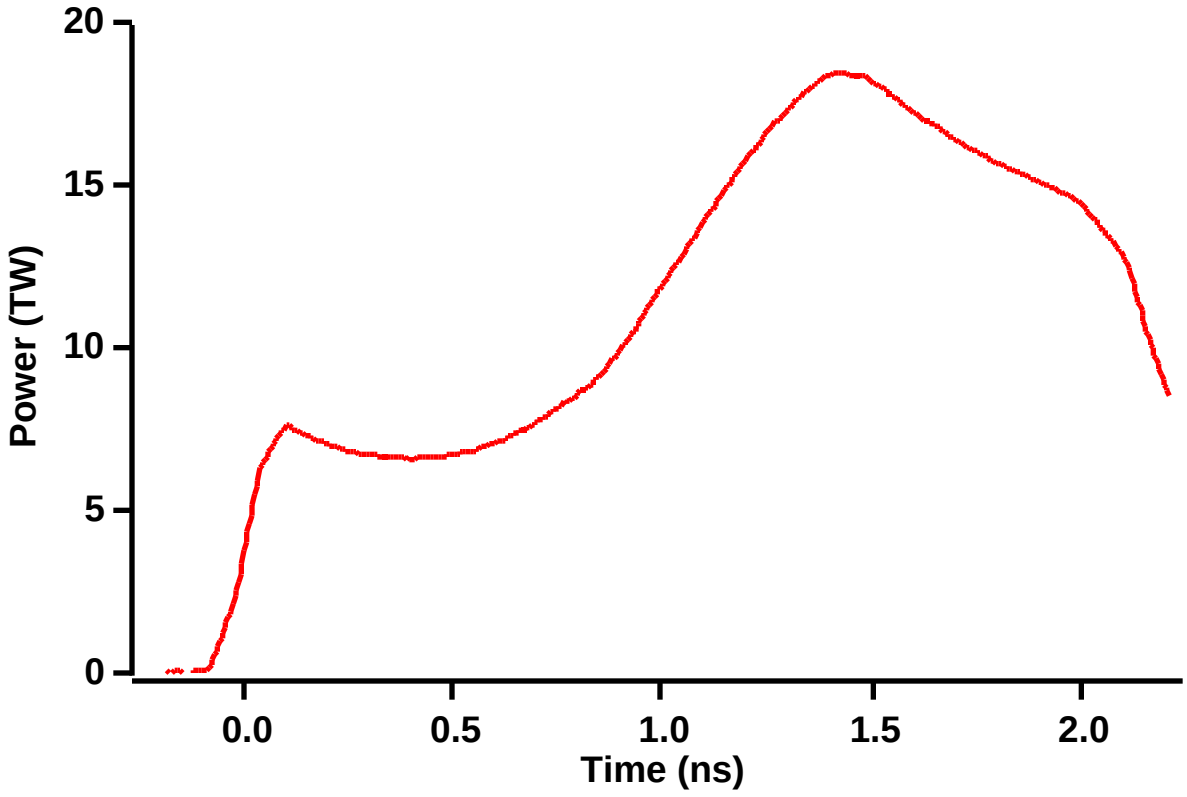

Figure 4: Pulse shape 22 as defined for Nova. The power is for the sum of all ten Nova beams.

The pointing is specified in a coordinate system in which the origin is at target chamber center. The z axis is along the ray from TCC through the center of the laser entrance hole. This ray and the ray from TCC to the center of the lens for the beam in question form a plane. The x axis is lies in this plane and is perpendicular to the z axis. The y axis is perpendicular to the x and z axes and the three form a right-handed coordinate system.

The pointing of each of the beams is determined by the position of best focus in this x, y, z coordinate system. From these values, the offsets for the beams can be determined.

Pulse shape

Two different pulse shapes will be used during the tetrahedral hohlraum campaign. The first will be a 1 ns flat top laser pulse.

The second laser pulse shape will be similar to that referred to on Nova as pulse shape 22 (PS22). This is a laser pulse with a duration of approximately 2.2 ns, consisting of a 0.7 ns foot, followed by a ramp up to a maximum at about 1.5 ns, and a subsequent fall. The contrast of this pulse shape is approximately 3 to 1.

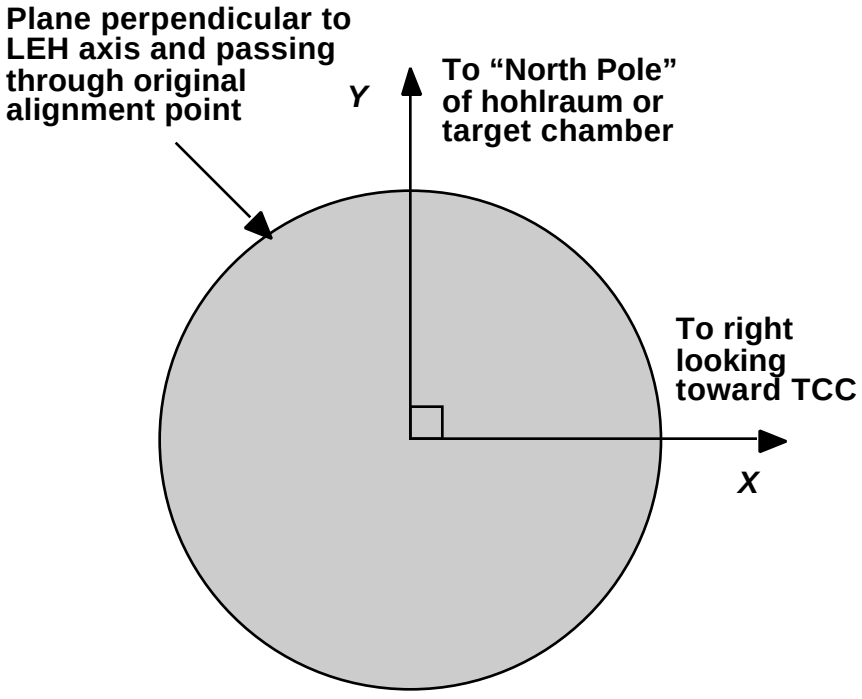

Figure 5: Definition of beam offsets used by LLE.

Beam pointing

Hohlraum orientation: H4–H7–H13–H20

LEH positions

LEH	Port	Theta	Phi
LEH A:	H4	37.4°	234°
LEH B:	H7	79.2°	90°
LEH C:	H13	100.8°	342°
LEH D:	H20	142.6°	198°

Beams in each beam cone

Cone A1a:	55, 46, 48	Cone C1a:	39, 16, 37
Cone A1b:	61, 52, 26	Cone C1b:	21, 35, 15
Cone A2a:	65, 17, 41	Cone C2a:	12, 34, 10
Cone A2b:	56, 60, 33	Cone C2b:	29, 27, 28
Cone A3:	22, 36, 40	Cone C3:	38, 31, 23
Cone B1a:	59, 18, 13	Cone D1a:	45, 44, 54
Cone B1b:	67, 66, 24	Cone D1b:	62, 64, 51
Cone B2a:	47, 14, 11	Cone D2a:	25, 42, 43
Cone B2b:	69, 68, 32	Cone D2b:	57, 19, 63
Cone B3:	50, 20, 58	Cone D3:	53, 49, 30

Beam alignment

The beams shall be aligned using a surrogate target centered on a point located along the laser entrance hole axis at a position 1356 μm from target chamber center. The beams will then be moved from those positions by an amount calculated separately for each beam and separately.

The pointing will be checked on a set of pointing experiments. The targets for these will be about 4000 μm (5/32 inch) plastic spheres with a thin gold coating. Low-energy shots will be performed and the x-ray emission from the lasers will be imaged using time-integrated pinhole cameras. The position of the spots will then be compared to the predicted positions, and any necessary corrections to be pointing will then be determined.

Target alignment

Targets will be aligned by rotating the target so that the alignment fiber on the stalk is pointed toward the y-axis target viewer and then centering the sphere in the x- and y- target viewers. Rotation adjustment will be specified as the rotation needed to bring the target into alignment; i.e. align the fiber and then rotate x degrees clockwise as viewed from above. Any necessary adjustments to centering due to rotation should then be made.

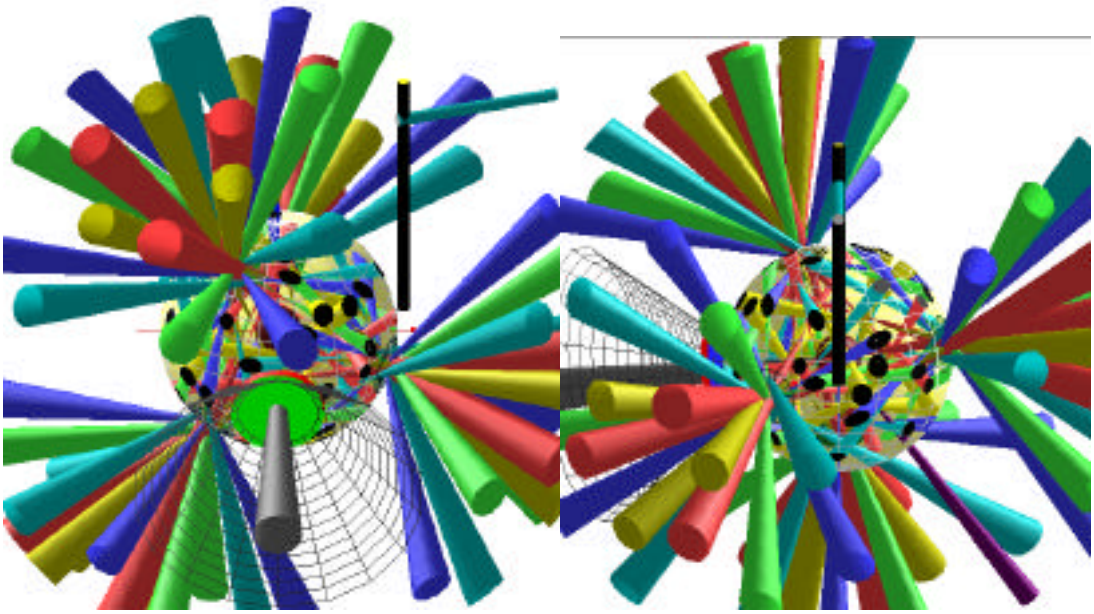

Figure 6: Target as seen in the X TVS (left) and Y TVS (right) when properly aligned. The open grid shows the location of the SOP shield for targets that have one and shows that the shield does not interfere with alignment.

Experiments to be performed

The experiments to be performed fall into three different types: double shell implosions, high-convergence implosions, and planar packages. In addition, pointing sphere targets will be used on the first day to verify beam pointing prior to the start of experiments.

Pointing sphere targets

The pointing targets will consist of 5/32" diameter plastic sphere targets with a ~1 μm Au coating. The targets will be mounted similarly to hohlraums, i.e. with a stalk connected to the equator of the sphere and an alignment fiber to set the rotation (Fig. 6).

These targets will be provided by LLE.

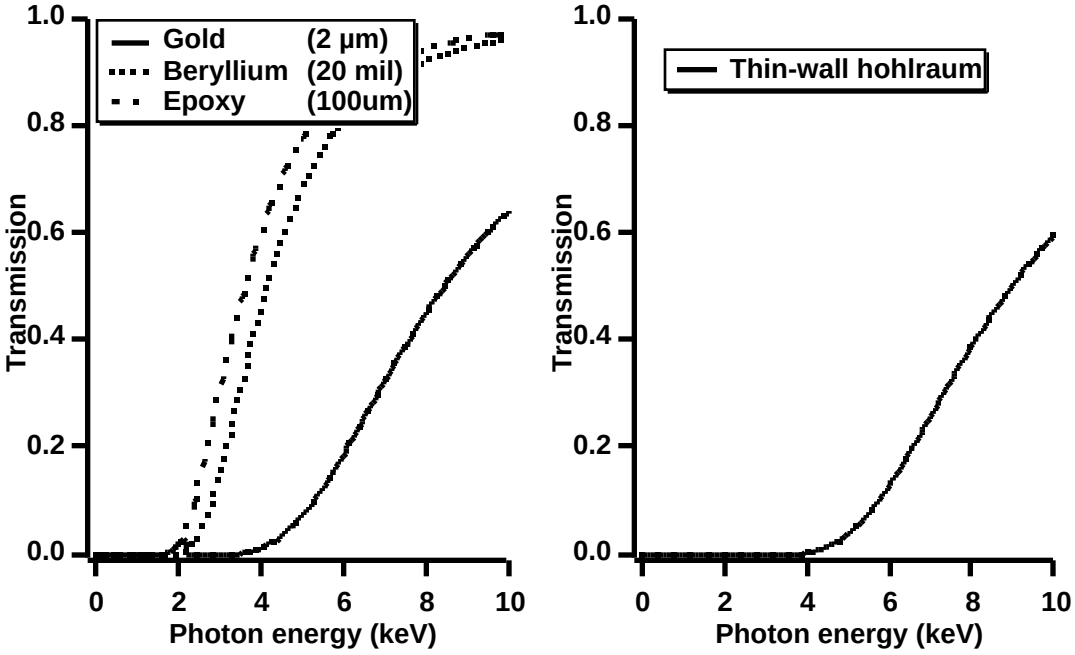

Figure 7: X-ray transmission of the components of a thin-wall hohlraum and the beryllium filter typically used in gated x-ray imagers (left) and the total transmission function (right). The transmission is dominated by the 2-μm gold layer of the hohlraum wall.

Double shell implosion targets

"Double-shell" targets will be tested during this series. These targets have previously been used on Nova experiments and at other facilities but have shown the same degradation in performance as seen in single-shell implosions. In this experiment, a determination will be made as to whether the improved time-dependent symmetry of in tetrahedral hohlraums will result in improved performance of this target design.

Six targets will used in this experiment, three with D_2 fill and three with DT fill. The primary diagnostics will be neutron-based. D_2 experiments will rely on Medusa to provide secondary neutron yield for determining ρR of the imploded fuel. DT will be used to allow high-accuracy neutron yield and burn history measurements.

Other than the type of fill, the targets will be identical. Assuming 10% yield compared to clean calculations, the yield from D_2 capsules will be about 7×10^7 DD neutrons, and about 3×10^{10} DT neutrons from DT-filled capsules.

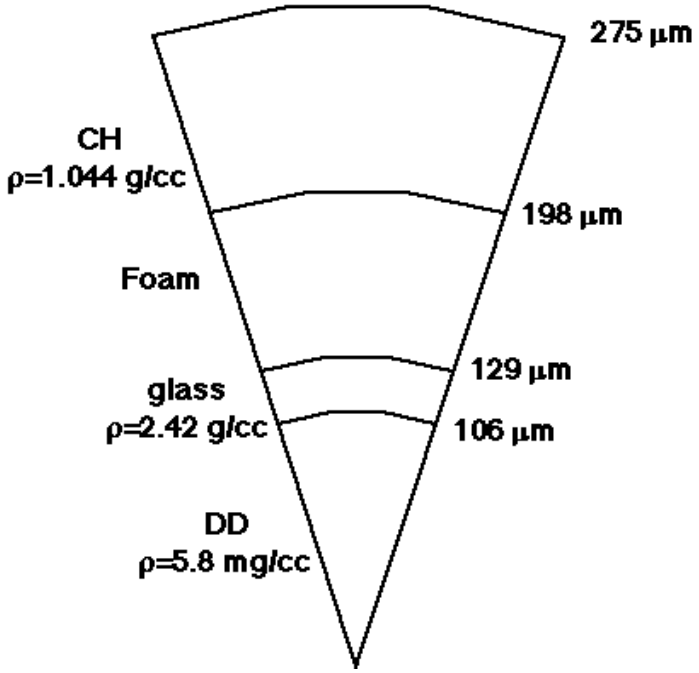

Figure 8: "Pie" diagram of a double-shell capsule. For half of the experiments, the inner capsule will be filled with D_2, and with DT for the other half.

High-convergence implosion targets

Standard implosion capsules are nominally 440 μm in inside diameter with a 55 μm thick plastic wall. They contain 50 atm D_2 and 0.1 atm Ar to allow x-ray imaging of the imploded core. By reducing the fill pressure, the final convergence of the capsule may be varied.

In this experiment, fill pressures of 8, 25, and 50 atm D_2 will be used. Two each of 8 atm and 25 atm targets will also contain 0.1 atm Ar to allow x-ray imaging of the imploded core. For experiments where neutron yield and neutron-based ρR measurements are to be made, capsules without Ar will be used.

A pre-shot report on the expected performance of these targets is included as an attachment to this report.

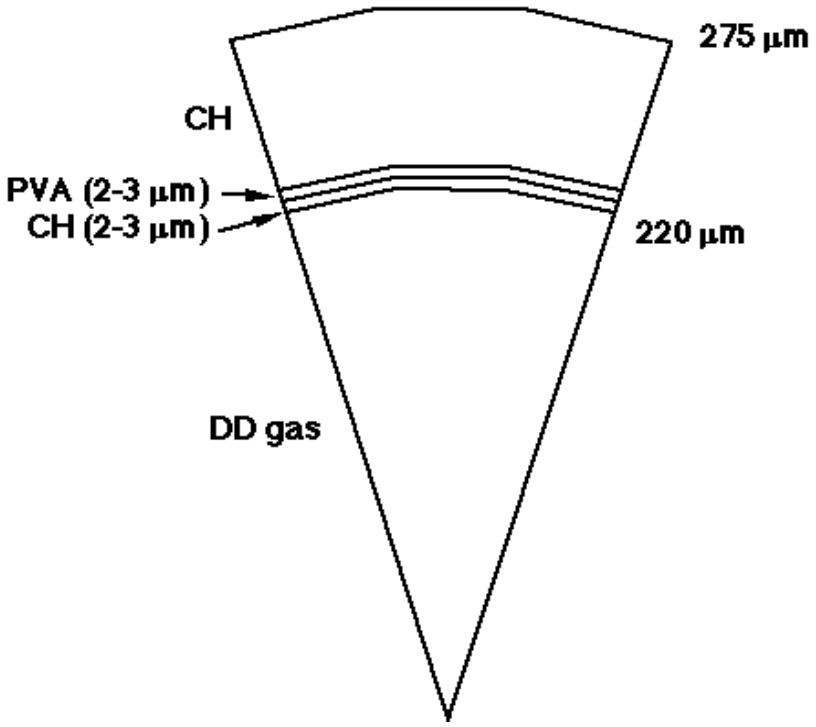

Figure 9: "Pie" diagram of a high-convergence capsule. The D_2 gas pressure will vary from 8 to 50 atm, and some of the capsules will contain 0.1 atm Ar to facilitate x-ray imaging.

Planar packages and SOP demonstration

A telescope has been constructed [10] for use as, among other things, a streaked optical pyrometer for measuring shock breakout from witness plates or planar packages mounted on hohlraums. A number of experiments will be conducted using this instrument.

Four targets will utilize flat witness plates to determine the uniformity of the drive on a planar package placed opposite a laser entrance hole in a tetrahedral hohlraum. Experiments will be performed using all 60 beams as well as with 45 beams only. For the 45 beam case, an iron foil will cover the LEH opposite the witness plate to simulate a backlighter foil that may be used in future experiments.

Two targets will use stepped witness plates and two will use wedged witness plates to demonstrate the utility of the Omega telescope for making radiation temperature measurements. Since radiation temperature is determined by measuring the shock speed in an aluminum plate, this

experiment will also demonstrate the ability to do shock speed measurements for future materials studies.

A final experiment will use the telescope to measure the effect of an aluminum joint on shock propagation through copper-doped beryllium. Be(Cu) is a leading ablator material candidate for NIF ignition hohlraums [11], but the effects on the implosion of a joint in two hemispheres need to be determined. This experiment will test the utility of the SOP for this type of experiment.

References

[1] C. Decker, R. E. Turner, O. L. Landen, L. J. Suter, P. Amendt, H. N. Kornblum, B. A. Hammel, T. J. Murphy, J. Wallace, N. D. Delamater, P. Gobby, A. A. Hauer, G. R. Magelssen, J. A. Oertel, J. Knauer, F. J. Marshall, D. Bradley, W. Seka, and J. M. Soures, Hohlraum radiation drive measurements on the Omega laser, *Phys. Rev. Lett.* **79**, 1491 (1997).

[2] T. J. Murphy, J. M. Wallace, N. D. Delamater, Cris W. Barnes, P. Gobby, A. A. Hauer, E. Lindman, G. Magelssen, J. B. Moore, J. A. Oertel, R. Watt, O. L. Landen, P. Amendt, M. Cable, C. Decker, B. A. Hammel, J. Koch, L. J. Suter, R. E. Turner, R. J. Wallace, F. J. Marshall, D. Bradley, R. S. Craxton, R. Keck, J. P. Knauer, R. Kremens, and J. D. Schnittman, Hohlraum symmetry experiments with multiple beam cones on the Omega Laser Facility, *Phys. Rev. Lett.* **81**, 108 (1998).

[3] T. J. Murphy, J. M. Wallace, N. D. Delamater, Cris W. Barnes, P. Gobby, A. A. Hauer, E. L. Lindman, G. Magelssen, J. B. Moore, J. A. Oertel, R. Watt, O. L. Landen, P. Amendt, M. Cable, C. Decker, B. A. Hammel, J. Koch, L. J. Suter, R. E. Turner, R. J. Wallace, F. J. Marshall, D. Bradley, R. S. Craxton, R. Keck, J. P. Knauer, R. Kremens, and J. D. Schnittman, Indirect drive experiments utilizing multiple beam cones in cylindrical hohlraums on OMEGA, *Phys. Plasmas* **5**, 1960 (1998).

[4] T. J. Murphy, J. Wallace, K. A. Klare, J. A. Oertel, C. W. Barnes, N. D. Delamater, P. Gobby, A. A. Hauer, E. Lindman, G. Magelssen, O. L. Landen, P. Amendt, C. Decker, L. Suter, B. Hammel, R. Turner, R. Wallace, R. S. Craxton, F. J. Marshall, D. Bradley, D. Harding, K. Kearney, R. Keck, J. Knauer, R. Kremens, W. Seka, M. Cable, and J. Schnittman, Experiments utilizing spherical hohlraums with tetrahedral illumination on Omega, *Bull. Am. Phys. Soc.* **42**, 2008 (1997).

[5] J. M. Wallace *et al.,* Measurements of radiative drive symmetry in tetrahedral hohlraums, to be published.

[6] J. D. Schnittman, R. S. Craxton, Indirect-drive radiation uniformity in tetrahedral hohlraums, *Phys. Plasmas* **3**, 3786 (1996).

[7] D. W. Phillion, S. M. Pollaine, Dynamical compensation of irradiation nonuniformities in a spherical hohlraum illuminated with tetrahedral symmetry, *Phys. Plasmas* **1**, 2963 (1995).

[8] T. J. Murphy, Tetrahedral Hohlraum Proof-of-Principle Experiments on Omega ID2, March 24-28, 1997 (unpublished).

[9] K. A. Klare, J. M. Wallace, and D. Drake, Tetrahedral hohlraum visualization and pointings, *Bull. Am. Phys. Soc.* **42**, 1993 (1997).

[10] J. A. Oertel, T. J. Murphy, R. R. Berggren, R. F. Horton, J. Faulkner, R. Schmell, D. Little, T. Archuleta, J. Lopez, and J. Velarde, A multipurpose TIM-based telescope for Omega and the Trident laser Facilities, submitted to *Rev. Sci. Instrum.*

[11] Douglas C. Wilson, Paul A. Bradley, Nelson M. Hoffman, Fritz J. Swenson, David P. Smitherman, Robert E. Chrien, Robert W. Margevicius, D. J. Thoma, Larry R. Foreman, James K. Hoffer, S. Robert Goldman, and Stephen E. Caldwell, Thomas R. Dittrich, Steven W. Haan, Michael M. Marinak, Stephen M. Pollaine, and Jorge J. Sanchez, The development and advantages of beryllium capsules for the National Ignition Facility, Phys. Plasmas 5, 1953 (1998).

Attachments

Shot plan overview

Detailed day-by-day shot plan

Diagnostic setup spreadsheets

Pointing parameters

Pointing offsets and pointing sphere positions

Target designs

High convergence pre-shot report

LLE area map

ID4-FY98 Shot Plan

Wednesday	Thursday	Friday
Pointing, double shell, test SOP	High Convergence Implosions	Planar packages 45 beams No beams to LEH B
Pointing	High Convergence (50 atm, no Argon)	Aluminum step witness plate
Pointing (if necessary)	High Convergence (50 atm, no Argon)	Aluminum step witness plate
Double Shell Implosion (DT)	High Convergence (25 atm with Argon)	Aluminum wedge witness plate
Double Shell Implosion (DT)	High Convergence (8 atm with Argon)	Aluminum wedge witness plate
Double Shell Implosion (DT)	High Convergence (8 atm with Argon)	BeCu plate, no joint
Double Shell Implosion (DD)	High Convergence (25 atm with Argon)	BeCu plate, with joint
Double Shell Implosion (DD)	High Convergence (25 atm No Argon)	
Double Shell Implosion (DD)	High Convergence (25 atm No Argon)	
Drive uniformity (60 beams)	High Convergence (8 atm No Argon)	
Drive uniformity (60 beams)	High Convergence (8 atm No Argon)	
Drive uniformity (45 beams; No beams to LEH B)	High Convergence (8 atm No Argon)	
Drive uniformity (45 beams; No beams to LEH B)	High Convergence (25 atm No Argon)	

1/6/99 10:34 AM

Overview: Summary for ID4-FY98 experiments for 2-4 September 1998

Targets:

All supplied by LANL EXCEPT pointing sphere targets (4 mm diameter from LLE)

Beamline Configuration:

Use 60 beams.
All beams:
Day 1: 1 ns square at 450 J/beam UVOT
Day 2: PS 22 at 340 J/beam UVOT
Day 3: 1 ns square at 450 J/beam UVOT

Timing: all beams start at t=0.

The last two shots on day one and all of day three will use only 45 beams.
Turn off the following beams:

11, 13, 14, 18, 20, 24, 32, 47, 50, 58, 59, 66, 67, 68, 69

Drive beams:

Tetrahedral pointing as previously supplied to LLE

Driver Configuration:
Day 1: 1 ns square at 450 J/beam UVOT
Day 2: PS 22 at 340 J/beam UVOT
Day 3: 1 ns square at 450 J/beam UVOT

Primary diagnostics
Secondary diagnostics

Varies from experiment to experiment,
See diagnostic setup sheets

	Mag	Delay	Interframe	Filtering	Bias	
Framing Camera #1 in TIM1	2 X	0.1 ns	250 ps	10 mil Be	200 volts	Monitor beam spots; Delay earlier for pointing experiments
Framing Camera #2 in TIM4	12 X	0.1 ns	250 ps	10 mil Be	0 volts	View implosion nearly perpendicular to LEH axis
Framing Camera #3 in TIM6, SXRFC snout	3 X	0.1 ns	250 ps	none	0 volts	Monitor Dante hole
Framing Camera #4 in TIM2	6 X	0.1 ns	250 ps	10 mil Be	100 volts	View implosion through LEH B

1 ns sq on all beams

Shot #	RID #	Target ID	Shot Description	Beamlines	Timing	Energy (J UV)	Pointing (mm)	Defocus (µm)	Target Type	TIM Diagnostics
1	4645	ID4-4Q98-PT-1	Pointing test TIM timing check	All 60	0 ns	100	Tetrahedral	Pointing Sphere Defocus	Pointing target 4 mm diameter	XRFC1@T1 t(0)-0.5 ns XRFC2@T4 t(0)-0.5 ns TIM-PHC @ T2 TIM-PHC @ T3 TIM-PHC @ T6 SOP @ T5
2	4646	ID4-4Q98-PT-2	Pointing test TIM timing check	All 60	0 ns	100	Tetrahedral	Pointing Sphere Defocus	Pointing target 4 mm diameter	XRFC1@T1 t(0)-0.5 ns XRFC2@T4 t(0)-0.5 ns TIM-PHC @ T2 TIM-PHC @ T3 TIM-PHC @ T6 SOP @ T5
3	4641	Dshell_DT-1 (3 black bands)	Double Shell Imp DT filled Expected Yield = 3 e 9 (1-D Yield = 2.8 e 10)	All 60	0 ns	450	Tetrahedral	Tetrahedral Defocus	Tetrahedral HR DT filled capsule	XRFC1@T1 t(0)+0.1 ns XRFC3@T6 t(0)+0.1 ns XRFC4@T2 t(0)+0.1 ns SOP @ T5
4	4642	Dshell_DT-2 (2 black bands)	Double Shell Imp DT filled Expected Yield = 3 e 9 (1-D Yield = 2.8 e 10)	All 60	0 ns	450	Tetrahedral	Tetrahedral Defocus	Tetrahedral HR DT filled capsule	XRFC1@T1 t(0)+0.1 ns XRFC3@T6 t(0)+0.1 ns XRFC4@T2 t(0)+0.1 ns SOP @ T5
5	4643	Dshell_DT-3 (1 black band)	Double Shell Imp DT filled Expected Yield = 3 e 9 (1-D Yield = 2.8 e 10)	All 60	0 ns	450	Tetrahedral	Tetrahedral Defocus	Tetrahedral HR DT filled capsule	XRFC1@T1 t(0)+0.1 ns XRFC3@T6 t(0)+0.1 ns XRFC4@T2 t(0)+0.1 ns SOP @ T5
6	4647	Dshell_DD-6 (1 silver band)	Double Shell Imp DD filled Expected Yield = 7 e 7 (1-D Yield = 7 e 8)	All 60	0 ns	450	Tetrahedral	Tetrahedral Defocus	Tetrahedral HR DD filled capsule	XRFC1@T1 t(0)+0.1 ns XRFC3@T6 t(0)+0.1 ns XRFC4@T2 t(0)+0.1 ns SOP @ T5
7	4648	Dshell_DD-7 (4 silver bands)	Double Shell Imp DD filled Expected Yield = 7 e 7 (1-D Yield = 7 e 8)	All 60	0 ns	450	Tetrahedral	Tetrahedral Defocus	Tetrahedral HR DD filled capsule	XRFC1@T1 t(0)+0.1 ns XRFC3@T6 t(0)+0.1 ns XRFC4@T2 t(0)+0.1 ns SOP @ T5
8	4649	Dshell_DD-8 (3 silver bands)	Double Shell Imp DD filled Expected Yield = 7 e 7 (1-D Yield = 7 e 8)	All 60	0 ns	450	Tetrahedral	Tetrahedral Defocus	Tetrahedral HR DD filled capsule	XRFC1@T1 t(0)+0.1 ns XRFC3@T6 t(0)+0.1 ns XRFC4@T2 t(0)+0.1 ns SOP @ T5
9	4622	OM_FLAT_60-1	Tetrahedral HR Flat witness plate	All 60	0 ns	450	Tetrahedral	Tetrahedral Defocus	Tetrahedral HR Witness plate SOP Shield	XRFC1@T1 t(0)+0.1 ns XRFC3@T6 t(0)+0.1 ns SOP @ T5
10	4623	OM_FLAT_60-2	Tetrahedral HR Flat witness plate	All 60	0 ns	450	Tetrahedral	Tetrahedral Defocus	Tetrahedral HR Witness plate SOP Shield	XRFC1@T1 t(0)+0.1 ns XRFC3@T6 t(0)+0.1 ns SOP @ T5
11	4624	OM_FLAT_45-1	Tetrahedral HR Flat witness plate	45 beams Turn off LEH B beams	0 ns	450	Tetrahedral	Tetrahedral Defocus	Tetrahedral HR Witness plate SOP Shield	XRFC1@T1 t(0)+0.1 ns XRFC3@T6 t(0)+0.1 ns SOP @ T5
12	4625	OM_FLAT_45-2	Tetrahedral HR Flat witness plate	45 beams Turn off LEH B beams	0 ns	450	Tetrahedral	Tetrahedral Defocus	Tetrahedral HR Witness plate SOP Shield	XRFC1@T1 t(0)+0.1 ns XRFC3@T6 t(0)+0.1 ns SOP @ T5

Thur 3 Sep 1998

	Mag	Delay	Interframe	Filtering	Bias	
Framing Camera #1 in TIM1	2 X	0.25 ns	500 ps	10 mil Be	200 volts	Monitor beam spots
Framing Camera #2 in TIM4	12 X	2.5 ns	250 ps	10 mil Be	100 V (no Ar) 200 V (w/Ar)	View implosion nearly perpendicular to
Framing Camera #3 in TIM6, SXRFC snout	3 X	0.25 ns	500 ps	none	0 volts	Monitor Dante hole
Framing Camera #4 in TIM2	12 X	2.5 ns	250 ps	10 mil Be	200 V (no Ar) 300 V (w/Ar)	View implosion through LEH B

PS22 on all beams

Shot #	RID #	Target ID	Shot Description	Beamlines	Timing	Energy (J UV)	Pointing (mm)	Defocus (μm)	Target Type	TIM Diagnostics
1	4396	GRB-HI-CON-1	High Convergence PS 22 50 atm DD/no Ar 16 yellow	All 60	0 ns	340	Tetrahedra	Tetrahedral Defocus	Tetrahedral HR Plastic Capsule	XRFC1@T1 t(0)+0.25 ns XRFC4@T2 t(0)+2.5 ns XRFC2@T4 t(0)+2.5 ns XRFC3@T6 t(0)+0.25 ns
2	4397	GRB-HI-CON-2	High Convergence PS 22 50 atm DD/no Ar 15 yellow	All 60	0 ns	340	Tetrahedra	Tetrahedral Defocus	Tetrahedral HR Plastic Capsule	XRFC1@T1 t(0)+0.25 ns XRFC4@T2 t(0)+2.5 ns XRFC2@T4 t(0)+2.5 ns XRFC3@T6 t(0)+0.25 ns
3	4398	GRB-HI-CON-3	High Convergence PS 22 25 atm DD/0.1 atm Ar 4 yellow	All 60	0 ns	340	Tetrahedra	Tetrahedral Defocus	Tetrahedral HR Plastic Capsule	XRFC1@T1 t(0)+0.25 ns XRFC4@T2 t(0)+2.5 ns XRFC2@T4 t(0)+2.5 ns XRFC3@T6 t(0)+0.25 ns
4	4399	GRB-HI-CON-4	High Convergence PS 22 8 atm DD/0.1 atm Ar 1yellow	All 60	0 ns	340	Tetrahedra	Tetrahedral Defocus	Tetrahedral HR Plastic Capsule	XRFC1@T1 t(0)+0.25 ns XRFC4@T2 t(0)+2.5 ns XRFC2@T4 t(0)+2.5 ns XRFC3@T6 t(0)+0.25 ns
5	4400	GRB-HI-CON-5	High Convergence PS 22 8 atm DD/0.1 atm Ar 2 yellow	All 60	0 ns	340	Tetrahedra	Tetrahedral Defocus	Tetrahedral HR Plastic Capsule	XRFC1@T1 t(0)+0.25 ns XRFC4@T2 t(0)+2.5 ns XRFC2@T4 t(0)+2.5 ns XRFC3@T6 t(0)+0.25 ns
6	4401	GRB-HI-CON-6	High Convergence PS 22 25 atm DD/0.1 atm Ar 6 yellow	All 60	0 ns	340	Tetrahedra	Tetrahedral Defocus	Tetrahedral HR Plastic Capsule	XRFC1@T1 t(0)+0.25 ns XRFC4@T2 t(0)+2.5 ns XRFC2@T4 t(0)+2.5 ns XRFC3@T6 t(0)+0.25 ns
7	4402	GRB-HI-CON-7	High Convergence PS 22 25 atm DD/No Ar 12 yellow	All 60	0 ns	340	Tetrahedra	Tetrahedral Defocus	Tetrahedral HR Plastic Capsule	XRFC1@T1 t(0)+0.25 ns XRFC4@T2 t(0)+2.5 ns XRFC2@T4 t(0)+2.5 ns XRFC3@T6 t(0)+0.25 ns
8	4403	GRB-HI-CON-8	High Convergence PS 22 25 atm DD/No Ar 13 yellow	All 60	0 ns	340	Tetrahedra	Tetrahedral Defocus	Tetrahedral HR Plastic Capsule	XRFC1@T1 t(0)+0.25 ns XRFC4@T2 t(0)+2.5 ns XRFC2@T4 t(0)+2.5 ns XRFC3@T6 t(0)+0.25 ns
9	4404	GRB-HI-CON-9	High Convergence PS 22 8 atm DD/No Ar 10 yellow	All 60	0 ns	340	Tetrahedra	Tetrahedral Defocus	Tetrahedral HR Plastic Capsule	XRFC1@T1 t(0)+0.25 ns XRFC4@T2 t(0)+2.5 ns XRFC2@T4 t(0)+2.5 ns XRFC3@T6 t(0)+0.25 ns
10	4405	GRB-HI-CON-10	High Convergence PS 22 8 atm DD/No Ar 7 yellow	All 60	0 ns	340	Tetrahedra	Tetrahedral Defocus	Tetrahedral HR Plastic Capsule	XRFC1@T1 t(0)+0.25 ns XRFC4@T2 t(0)+2.5 ns XRFC2@T4 t(0)+2.5 ns XRFC3@T6 t(0)+0.25 ns
11	4406	GRB-HI-CON-11	High Convergence PS 22 8 atm DD/No Ar 9 yellow	All 60	0 ns	340	Tetrahedra	Tetrahedral Defocus	Tetrahedral HR Plastic Capsule	XRFC1@T1 t(0)+0.25 ns XRFC4@T2 t(0)+2.5 ns XRFC2@T4 t(0)+2.5 ns XRFC3@T6 t(0)+0.25 ns
12	4407	GRB-HI-CON-12	High Convergence PS 22 25 atm DD/No Ar 11 yellow	All 60	0 ns	340	Tetrahedra	Tetrahedral Defocus	Tetrahedral HR Plastic Capsule	XRFC1@T1 t(0)+0.25 ns XRFC4@T2 t(0)+2.5 ns XRFC2@T4 t(0)+2.5 ns XRFC3@T6 t(0)+0.25 ns
13	4408	GRB-HI-CON-13	High Convergence PS 22 8 atm DD/0.1 atm Ar 3 yellow	All 60	0 ns	340	Tetrahedra	Tetrahedral Defocus	Tetrahedral HR Plastic Capsule	XRFC1@T1 t(0)+0.25 ns XRFC4@T2 t(0)+2.5 ns XRFC2@T4 t(0)+2.5 ns XRFC3@T6 t(0)+0.25 ns

Fri 4 Sep 1998

	Mag	Delay	Interframe	Filtering	Bias	
Framing Camera#1 in TIM1	2 X	0.1 ns	250 ps	10 mil Be	200 volts	Monitor beam spots
Framing Camera #3 in TIM6, SXRFC snout	3 X	0.1 ns	250 ps	none	0 volts	Monitor Dante hole

1 ns sq on all beams

Shot #	RID #	Target ID	Shot Description	Beamlines	Timing	Energy (J UV)	Pointing (mm)	Defocus (µm)	Target Type	TIM Diagnostics
1	4624	OM_FLAT_45-1	Tetrahedral HR Flat witness plate	45 beams Turn off LEH B beams	0 ns	500	Tetrahedral	Tetrahedral Defocus	Tetrahedral HR Witness plate SOP Shield	XRFC1@T1 t(0)+0.1 ns XRFC3@T6 t(0)+0.1 ns SOP @ T5
2	4626	OM_WEDGE_45-1	Tetrahedral HR Wedge witness plate	45 beams Turn off LEH B beams	0 ns	500	Tetrahedral	Tetrahedral Defocus	Tetrahedral HR Witness plate SOP Shield	XRFC1@T1 t(0)+0.1 ns XRFC3@T6 t(0)+0.1 ns SOP @ T5
3	4628	OM_STEP_45-1	Tetrahedral HR Step witness plate	45 beams Turn off LEH B beams	0 ns	500	Tetrahedral	Tetrahedral Defocus	Tetrahedral HR Witness plate SOP Shield	XRFC1@T1 t(0)+0.1 ns XRFC3@T6 t(0)+0.1 ns SOP @ T5
4	4651	OM_JOINT_45_1	Tetrahedral HR BeCu plate w/Al join	45 beams Turn off LEH B beams	0 ns	500	Tetrahedral	Tetrahedral Defocus	Tetrahedral HR Witness plate SOP Shield	XRFC1@T1 t(0)+0.1 ns XRFC3@T6 t(0)+0.1 ns SOP @ T5
5	4630	OM_FLATBE_45-1	Tetrahedral HR BeCu plate	45 beams Turn off LEH B beams	0 ns	500	Tetrahedral	Tetrahedral Defocus	Tetrahedral HR Witness plate SOP Shield	XRFC1@T1 t(0)+0.1 ns XRFC3@T6 t(0)+0.1 ns SOP @ T5
6	4627	OM_WEDGE_45-2	Tetrahedral HR Wedge witness plate	45 beams Turn off LEH B beams	0 ns	500	Tetrahedral	Tetrahedral Defocus	Tetrahedral HR Witness plate SOP Shield	XRFC1@T1 t(0)+0.1 ns XRFC3@T6 t(0)+0.1 ns SOP @ T5
7	4629	OM_STEP_45-1	Tetrahedral HR Step witness plate	45 beams Turn off LEH B beams	0 ns	500	Tetrahedral	Tetrahedral Defocus	Tetrahedral HR Witness plate SOP Shield	XRFC1@T1 t(0)+0.1 ns XRFC3@T6 t(0)+0.1 ns SOP @ T5
8	4631	OM_FLATBE_45-2	Tetrahedral HR BeCu plate	45 beams Turn off LEH B beams	0 ns	500	Tetrahedral	Tetrahedral Defocus	Tetrahedral HR Witness plate SOP Shield	XRFC1@T1 t(0)+0.1 ns XRFC3@T6 t(0)+0.1 ns SOP @ T5
9	4652	S2-4Q98-TRB038-	Disk with Grid	59, 66, 67	0 ns	500	tcc	+600 µm	Disk with grid	SOP @ T5
10	4653	OM_DISK-1	Gold disk	41	0 ns	500	tcc	+600 µm	Gold disk	SOP @ T5

Diagnostic setup sheet

Campaign: ID4-FY98 Tetrahedral Hohlraums

Day:	**1**	**Pulse shape:**	**1 ns square**	
Shots:	**1, 2**	**Energy/beam (UVOT):**	**100**	**J**
PI:	**Delamater**	**Beams on Target:**	**60**	
		Total Energy on Target:	**6**	**kJ**

Target: 4 mm pointing sphere
Alignment: Centered with fidu pointing at Y TVS

Purpose: check pointing and time instruments

TIM-based diagnostics

TIM		Instrument	Pri.	Magnification	Pinholes	Filtering	Timing	Strip Timing	Bias	Notes
1	P3	XRFC1	2	2	10 µm	10 mil Be	To - 0.5 ns	250 ps	+200 V	Time instrument
2	H7	TIM-based PHC	1	4	10 µm	5 mil Be				Pointing verification
3	H18	TIM-based PHC	1	4	10 µm	5 mil Be				Pointing verification
4	P6	XRFC2	2	12	5 µm	10 mil Be	To - 0.5 ns	250 ps	+200 V	Time instrument
5	H14	SOP	2							see John Oertel for setup
6	P7	TIM-based PHC	1	4	10 µm	5 mil Be				Pointing verification

Fixed x-ray diagnostics			Pri.	Magnification	Pinholes	Filtering	Timing	Strip Timing	Bias	Notes
KBs	H8F	KB1	not used							
	H9F	KB2/GMXI	2	13		No additional	To - 0.2 ns			Time instrument
	H13F	KB3	not used							
PHCs	P12A	XRPHC #1	1	4	10 µm	6 mil Be				Pointing verification
	H9C	XRPHC #2	1	4	10 µm	6 mil Be				Pointing verification
	H8C	XRPHC #3	1	4	10 µm	6 mil Be				Pointing verification
	H3C	XRPHC #4	1	4	10 µm	6 mil Be				Pointing verification
	H13C	XRPHC #5	1	4	10 µm	6 mil Be				Pointing verification
	H12C	XRPHC #6	1	4	10 µm	6 mil Be				Pointing verification
Dante	H16I	Dante	2							Time Dante
IXRSC	H3F	Imaging x-ray streak	2							

Neutron Diagnostics		Pri.	Type	Expected Yield	Bang time	Notes
H15D	LANL Bangtime	2	x rays	–	0.5 ns	Neutron bang time for testing and timing
P2D	LLE Bangtime	2	x rays	–	0.5 ns	Look for x-rays to confirm timing

Laser Diagnostics

P510A streaks	**Clusters 4 & 5**
Pulseshape measurements	**Beams 19 & 20**

Diagnostic setup sheet

Campaign: ID4-FY98 Tetrahedral Hohlraums

Day:	**1**	**Pulse shape:**	**1 ns square**		
Shots:	**3—8**	**Energy/beam (UVOT):**	**450**	**J**	
PI:	**Watt**	**Beams on Target:**	**60**		
		Total Energy on Target:	**27**	**kJ**	**(would prefer 28 kJ)**

Target: Tetrahedral hohlraum with double-shell capsule
Alignment: Centered with fidu pointing at Y TVS

Purpose: Measure performance of double-shell implosions in tetrahedral hohlraums

TIM-based diagnostics

TIM		Instrument	Pri.	Magnification	Pinholes	Filtering	Timing	Strip Timing	Bias	Notes
1	P3	XRFC1	2	2	10 μm	10 mil Be	To + 0.1 ns	250 ps	+200 V	Monitor Laser Spots
2	H7	XRFC4	2	6	10 μm	10 mil Be	To + 0.1 ns	250 ps	+100 V	View implosion through LEH B
3	H18	none								
4	P6	none								
5	H14	SOP	2							see John Oertel for setup; shakedown for following shots
6	P7	XRFC3/SXRFC snout	2	3	25/10/25		To + 0.1 ns	250 ps		Monitor Dante Hole (LEH D), X=-808 μm, Y=-263 μm, Z=-1113 μm

Fixed x-ray diagnostics			Pri.	Magnification	Pinholes	Filtering	Timing	Strip Timing	Bias	Notes
KBs	H8F	KB1	not used							
	H9F	KB2/GMXI	not used							
	H13F	KB3	not used							
PHCs	P12A	XRPHC #1	2	4	10 μm	6 mil Be				
	H9C	XRPHC #2	2	4	10 μm	6 mil Be				
	H8C	XRPHC #3	2	4	10 μm	6 mil Be				
	H3C	XRPHC #4	2	4	10 μm	6 mil Be				
	H13C	XRPHC #5	2	4	10 μm	6 mil Be + 0.5 mil Al				View implosion through LEH C
	H12C	XRPHC #6	2	4	10 μm	6 mil Be				
Dante	H16I	Dante	2							Test Dante settings, assume 200 eV peak
IXRSC	H3F	Imaging x-ray streak	2							

Neutron Diagnostics		Pri.	Type	Expected Yield	Bang Time	Notes
P10	Medusa/nToF	1				Secondary DT yield
P12B	Neutron scintillator	1	for DD-filled capsules:			Primary DD yield
P9A	Indium activation	1	DD	7 X 10^7	2.3 ns	Primary DD yield
P9C	Copper activation	1				Primary DT yield
	Mike Cable's nToF	1	for DT-filled capsules:			Ion temperature
P2D	LLE Bangtime	1	DT	3 X 10^9	2.3 ns	Neutron bang time
H15D	LANL Bangtime	1				Neutron bang time
H5I	nTD	1				Neutron burn history on DT shots

Laser Diagnostics

P510A streaks	**Clusters 4 & 5**
Pulseshape measurements	**Beams 19 & 20**

Diagnostic setup sheet

Campaign: ID4-FY98 Tetrahedral Hohlraums

Day:	**1**	**Pulse shape:**	**1 ns square**			
Shots:	**9—12**	**Energy/beam (UVOT):**	**450**	**J**	**450**	**J**
PI:	**Kyrala**	**Beams on Target:**	**60**		**45**	
		Total Energy on Target:	**27**	**kJ**	**20.25**	**kJ**
			Shots 9, 10		**Shots 11, 12**	

<<< on last two targets

Target: Tetrahedral hohlraum with witness plate
Alignment: Centered with fidu pointing at Y TVS

Purpose: check pointing and time instruments

TIM-based diagnostics

TIM		Instrument	Pri.	Magnification	Pinholes	Filtering	Timing	Strip Timing	Bias	Notes
1	P3	XRFC1		2	10 μm	10 mil Be	To + 0.1 ns	250 PS	+200 V	Monitor Laser Spots
2	H7	none								
3	H18	none								
4	P6	none								
5	H14	SOP	1							see John Oertel for setup
6	P7	XRFC3/SXRFC snout	1	3	25/10/25		To + 0.1 ns	250 ps		Monitor Dante Hole (LEH D), X=-808 μm, Y=-263 μm, Z=-1113 μm

Fixed x-ray diagnostics			Pri.	Magnification	Pinholes	Filtering	Timing	Strip Timing	Bias	Notes
KBs	H8F	KB1	not used							
	H9F	KB2/GMXI	not used							
	H13F	KB3	not used							
PHCs	P12A	XRPHC #1	2	4	10 μm	6 mil Be				
	H9C	XRPHC #2	2	4	10 μm	6 mil Be				
	H8C	XRPHC #3	2	4	10 μm	6 mil Be				
	H3C	XRPHC #4	2	4	10 μm	6 mil Be				
	H13C	XRPHC #5	2	4	10 μm	6 mil Be				
	H12C	XRPHC #6	2	4	10 μm	6 mil Be				
Dante	H16I	Dante	1							Measure x-ray drive, assume 200 eV peak (60 beams), 185 eV (45 beams)
IXRSC	H3F	Imaging x-ray streak	2							

Neutron Diagnostics	Pri.	Type	Expected Yield	Bang time	Notes
none					

Laser Diagnostics

P510A streaks	Clusters 4 & 5
Pulseshape measurements	Beams 19 & 20

Diagnostic setup sheet

Campaign: ID4-FY98 Tetrahedral Hohlraums

Day:	**2**	**Pulse shape:**	**PS 22**	
Shots:	**1—12**	**Energy/beam (UVOT):**	**340**	**J**
PI:	**Bennett**	**Beams on Target:**	**60**	
		Total Energy on Target:	**20.4**	**kJ**

Target: Tetrahedral hohlraum with capsule
Alignment: Centered with fidu pointing at Y TVS

Purpose: achieve high convergence in a tetrahedral hohlraum

TIM-based diagnostics

TIM		Instrument	Pri.	Magnification	Pinholes	Filtering	Timing	Strip Timing	Bias	Notes
1	P3	XRFC1	2	2	10 μm	10 mil Be	To + 0.25 ns	500 ps	+200 V	Monitor Laser Spots
2	H7	XRFC4	1	12	5 μm	10 mil Be	To + 2.5 ns	250 ps	+300 V	View implosion through LEH B
3	H18	TIM-based PHC	2	12	3 x 5 μm	10 mil Be	—	—		View implosion through wall
4	P6	XRFC2	1	12	5 μm	10 mil Be	To + 2.5 ns	250 ps	+200 V	View implosion through wall nearly perpendicular to axis
5	H14	SOP								
6	P7	XRFC3/SXRFC snout	2	3	25/10/25		To + 0.25 ns	500 ps		Monitor Dante Hole (LEH D), X=-808 μm, Y=-263 μm, Z=-1113 μm

Fixed x-ray diagnostics			Pri.	Magnification	Pinholes	Filtering	Timing		Notes
KBs	H8F	KB1	2	13		no additional			with grating
	H9F	KB2/GMXI	2	13		no additional	To + 2.3 ns	500 ps	crystal removed
	H13F	KB3	1	20		none on 1&2, 1 mil Al on 3&4			View implosion through LEH C, grating removed
PHCs	P12A	XRPHC #1	2	4	10 μm	6 mil Be			
	H9C	XRPHC #2	2	4	10 μm	6 mil Be			
	H8C	XRPHC #3	2	4	10 μm	6 mil Be			
	H3C	XRPHC #4	2	4	10 μm	6 mil Be			
	H13C	XRPHC #5	1	4	10 μm	6 mil Be + 0.5 mil Al			View implosion through LEH C
	H12C	XRPHC #6	2	4	10 μm	6 mil Be			
Dante	H16I	Dante	2						Monitor Dante traces
IXRSC	H3F	Imaging x-ray streak	2						

Neutron Diagnostics		Pri.	Type	Expected Yield	Bang time	Notes
P10	Medusa/nToF	1				Secondary DT yield
P12B	Neutron scintillator	1	DD	0.8 to 5 x 10^8	3. 0 ns	Primary DD yield
P9A	Indium activation	2				Primary DD yield
	Mike Cable's nToF	1				Ion temperature
P2D	LLE Bangtime	2				Neutron bang time, plan for 3 ns
H15D	LANL Bangtime	1				Neutron bang time, plan for 3 ns

Laser Diagnostics

P510A streaks	Clusters 4 & 5
Pulseshape measurements	Beams 19 & 20

Diagnostic setup sheet

Campaign: ID4-FY98 Tetrahedral Hohlraums

Day:	**3**	**Pulse shape:**	**1 ns square**	
Shots:	**1—6**	**Energy/beam (UVOT):**	**450**	**J**
PI:	**Kyrala**	**Beams on Target:**	**45**	
		Total Energy on Target:	**20.25**	**kJ**

Target: Tetrahredral hohlraum with witness plate or planar package
Alignment: Centered with fidu pointing at Y TVS

Purpose: test use of planar packages with tetrahedral hohlraums

TIM-based diagnostics

TIM		Instrument	Pri.	Magnification	Pinholes	Filtering	Timing	Strip Timing	Bias	Notes
1	P3	XRFC1	2	2	10 μm	10 mil Be	To + 0.1 ns	250 ps	+200 V	Monitor Laser Spots
2	H7	none								
3	H18	none								
4	P6	none								
5	H14	SOP	1							see J. Oertel for setup
6	P7	XRFC3/SXRFC snout	1	3	25/10/25		To + 0.1 ns	250 ps		Monitor Dante Hole (LEH D), X=-808 μm, Y=-263 μm, Z=-1113 μm

Fixed x-ray diagnostics			Pri.	Magnification	Pinholes	Filtering	Timing	Strip Timing	Bias	Notes
KBs	H8F	KB1	not used							
	H9F	KB2/GMXI	not used							
	H13F	KB3	not used							
PHCs	P12A	XRPHC #1	2	4	10 μm	6 mil Be				View target from various angles
	H9C	XRPHC #2	2	4	10 μm	6 mil Be				View target from various angles
	H8C	XRPHC #3	2	4	10 μm	6 mil Be				View target from various angles
	H3C	XRPHC #4	2	4	10 μm	6 mil Be				View target from various angles
	H13C	XRPHC #5	2	4	10 μm	6 mil Be				View target from various angles
	H12C	XRPHC #6	2	4	10 μm	6 mil Be				View target from various angles
Dante	H16I	Dante	1							Measure x-ray drive, assume 185 eV peak
IXRSC	H3F	Imaging x-ray streak	2							

Neutron Diagnostics	Pri.	Type	Expected Yield	Bang time	Notes
none					

Laser Diagnostics

P510A streaks	Clusters 4 & 5
Pulseshape measurements	Beams 19 & 20

Pointing Parameters

	LEH A	LEH B	LEH C	LEH D
Port:	H4	H7	H13	H20
Theta:	37.377	79.188	100.812	142.623
Phi:	234	90	342	198

Position of surrogate for initial beam pointing (prior to offsets):

Distance from TCC: 1356 µm

	LEH A	LEH B	LEH C	LEH D
X	-484	0	1267	-783
Y	-666	1332	-412	-254
Z	1078	254	-254	-1078

Klare coordinates for beam pointing:

Scale-1.2 pointing

	x	y	z
1A	525	-45	256
1B	370	-50	700
2A	455	20	1035
2B	375	-170	1000
3	110	-50	1278

Tetrahedral Pointing Parameters

0.0175

config: 407

LEH	Port	Theta	Phi	s	unit hole vector -- kk z X	Y	Z	1400 µm from TCC X	Y	Z	sample offsets R(LEH) 500 X	Y	Z
requires beam reassignment													
A	4	37.377	234		-0.357	-0.491	0.795	-500	-688	1113	460	-190	256
B	7	79.188	90		0.000	0.982	0.188	0	1375	263	370	-50	700
C	13	100.81	342		0.934	-0.304	-0.188	1308	-425	-263	570	-50	1035
D	20	142.62	198		-0.577	-0.188	-0.795	-808	-263	-1113	375	-170	1000
											110	-50	1278

"Try4" positions for Scale-1.2 pointing

CURRENT DISPLAY

Cone	Angle	R(LEH) 350 X	Y	Z	LEH center 1355.5 µm from TCC X	Y	Z	R(LEH) 350 X	Y	Z
1A	23.20	525	-45	256				525	-45	256
1B	23.20	370	-50	700	-484	-666	1077	370	-50	700
2A	47.83	455	20	1035	0	1331	254	455	20	1035
2B	47.83	375	-170	1000	1266	-411	-254	375	-170	1000
3	58.79	110	-50	1278	-783	-254	-1077	110	-50	1278

R retro 1356 RRRmax 170.96 1998

LEH	Cone	Beam	Beam Theta	Beam Phi	kk y	Focus wrt TCC X	Y	Z	Retro Dead Recon Offset XXX	YYY	ZZZ	Check Sphere theta	phi	ZZZZ
A	1A	55	42.0	198.0		297	-479	159	51	-48	1197	38.8	-136.1	-685
A	1A	46	21.4	270.0		-547	-203	-49	-67	-20	1197	31.5	-121.6	-685
A	1A	48	58.9	246.1		-24	305	500	16	68	1197	42.5	-120.1	-685
A	1B	61	21.4	198.0		-278	-655	351	6	-102	714	34.0	-133.3	-689
A	1B	52	58.9	221.9		66	-271	743	85	56	714	42.7	-127.6	-689
A	1B	26	42.0	270.0		-537	-105	575	-91	45	714	36.0	-117.2	-689
A	2A	65	58.9	174.1		15	-752	845	100	24	478	40.0	-150.4	-850
A	2A	17	21.4	342.0		-720	-658	573	-29	-98	478	25.1	-107.7	-850
A	2A	41	81.2	257.5		-403	-115	1050	-70	75	478	51.2	-116.2	-850
A	2B	56	21.4	126.0		-528	-770	545	-159	-64	530	26.7	-155.2	-802
A	2B	60	81.2	210.5		27	-547	933	134	-106	530	55.4	-132.3	-802
A	2B	33	58.9	293.9		-569	-157	906	24	169	530	37.0	-95.1	-802
A	3_	22	21.4	54.0		-548	-669	949	-50	19	151	13.8	-132.0	-914
A	3_	36	81.2	282.5		-467	-523	1075	41	34	151	51.7	-98.7	-914
A	3_	40	81.2	185.5		-353	-691	1023	9	-53	151	53.6	-150.6	-914
B	1A	59	81.2	113.5		522	238	119	-51	48	1197	78.3	96.4	-685
B	1A	18	98.8	77.5		-324	173	456	67	20	1197	85.1	87.7	-685
B	1A	13	58.9	77.9		-198	343	-432	-16	-68	1197	74.3	85.9	-685
B	1B	67	98.8	102.5		160	624	463	-6	102	714	82.8	94.1	-689
B	1B	66	58.9	102.1		213	745	-170	-85	-56	714	73.9	91.1	-689
B	1B	24	81.2	66.5		-372	693	101	91	-45	714	80.9	84.8	-689
B	2A	47	81.2	138.5		454	1023	158	-100	-24	478	79.6	105.6	-850
B	2A	14	121.1	66.1		-196	939	598	29	98	478	92.5	82.4	-850
B	2A	11	42.0	54.0		-258	1087	-174	70	-75	478	66.0	81.7	-850
B	2B	69	121.1	113.9		26	905	591	159	64	530	92.8	102.7	-802
B	2B	68	42.0	126.0		343	1025	-36	-134	106	530	61.5	95.9	-802
B	2B	32	81.2	41.5		-369	1017	7	-24	-169	530	84.0	71.9	-802
B	3_	50	138.0	90.0		-50	1235	348	50	-19	151	102.8	91.5	-914
B	3_	20	58.9	30.1		-70	1274	143	-41	-34	151	69.7	67.4	-914
B	3_	58	58.9	149.9		120	1258	228	-9	53	151	67.0	111.3	-914
C	1A	39	121.1	354.1		265	-295	432	16	68	1197	105.7	-13.9	-685
C	1A	16	98.8	318.5		388	423	-119	51	-48	1197	101.7	-24.4	-685
C	1A	37	81.2	354.5		65	-361	-456	-67	-20	1197	94.9	-15.7	-685
C	1B	21	121.1	329.9		774	-28	170	85	56	714	106.1	-19.1	-689
C	1B	35	98.8	5.5		544	-568	-101	-91	45	714	99.1	-12.8	-689
C	1B	15	81.2	329.5		643	-41	-463	6	-102	714	97.2	-22.1	-689
C	2A	12	138.0	18.0		954	-582	174	-70	75	478	114.0	-9.7	-850
C	2A	34	98.8	293.5		1114	116	-158	100	24	478	100.4	-33.6	-850
C	2A	10	58.9	5.9		833	-476	-598	-29	-98	478	87.5	-10.4	-850
C	2B	29	138.0	306.0		1081	10	36	134	-106	530	118.5	-23.9	-802
C	2B	27	98.8	30.5		853	-665	-7	24	169	530	96.0	0.1	-802
C	2B	28	58.9	318.1		869	-255	-591	-159	-64	530	87.2	-30.7	-802
C	3_	38	121.1	282.1		1233	-274	-228	9	-53	151	113.0	-39.3	-914
C	3_	31	42.0	342.0		1159	-429	-348	-50	19	151	77.2	-19.5	-914
C	3_	23	121.1	41.9		1190	-460	-143	41	34	151	110.3	4.6	-914
D	1A	45	158.6	162.0		-362	-458	49	67	20	1197	148.5	-166.4	-685
D	1A	44	121.1	185.9		282	-117	-500	-16	-68	1197	137.5	-167.9	-685
D	1A	54	138.0	234.0		-364	431	-159	-51	48	1197	141.2	-151.9	-685
D	1B	62	138.0	162.0		-266	-478	-575	91	-45	714	144.0	-170.8	-689
D	1B	64	158.6	234.0		-709	-62	-351	-6	102	714	146.0	-154.7	-689
D	1B	51	121.1	210.1		-238	146	-743	-85	-56	714	137.3	-160.4	-689
D	2A	25	158.6	90.0		-848	-481	-573	29	98	478	154.9	179.7	-850
D	2A	42	98.8	174.5		-234	-348	-1050	70	-75	478	128.8	-171.8	-850
D	2A	43	121.1	257.9		-710	247	-845	-100	-24	478	140.0	-137.6	-850
D	2B	57	121.1	138.1		-325	-493	-906	-24	-169	530	143.0	167.1	-802
D	2B	19	158.6	306.0		-896	-264	-545	159	64	530	153.3	-132.8	-802
D	2B	63	98.8	221.5		-511	195	-933	-134	106	530	124.6	-155.7	-802
D	3_	53	98.8	149.5		-642	-282	-1075	-41	-34	151	128.3	170.7	-914
D	3_	49	98.8	246.5		-766	-122	-1023	-9	53	151	126.4	-137.4	-914
D	3_	30	158.6	18.0		-806	-314	-949	50	-19	151	166.2	-156.0	-914

LEH Coordinates:

LEH	Theta	Phi
LEH A:	37.38	234
LEH B:	79.19	90
LEH C:	100.81	342
LEH D:	142.62	198
Stalk attachment:	90.00	20
Fidu wire alignment:		20

Tetrahedral Hohlraums for Omega
H4-H7 orientation

Tom Murphy
July 20, 1998

(not drawn to scale)

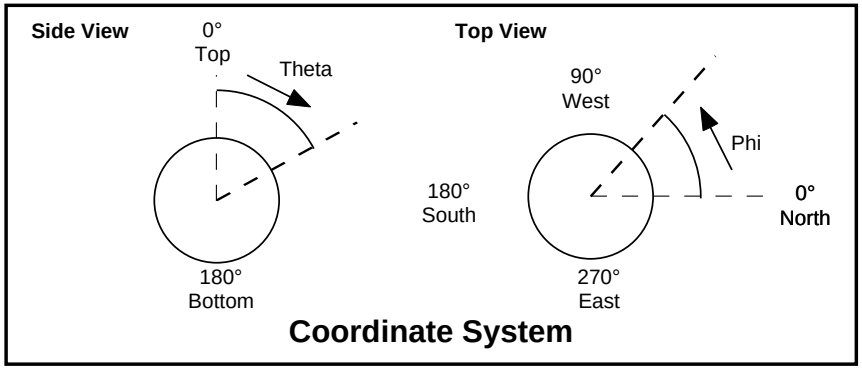

Coordinate System

Thin-wall hohlraums

Inside diameter:	2800 µm
LEH diameter:	700 µm
Gold Thickness:	2 µm
CH Thickness:	100 µm

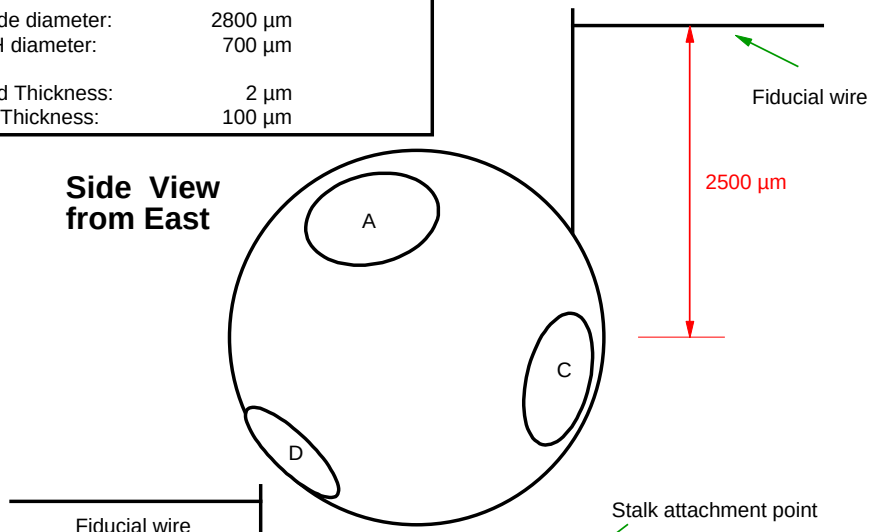

Side View from East

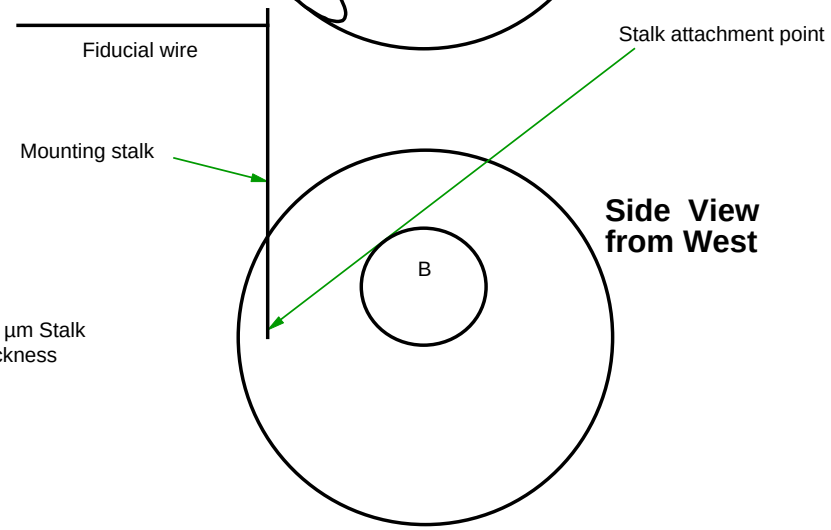

Side View from West

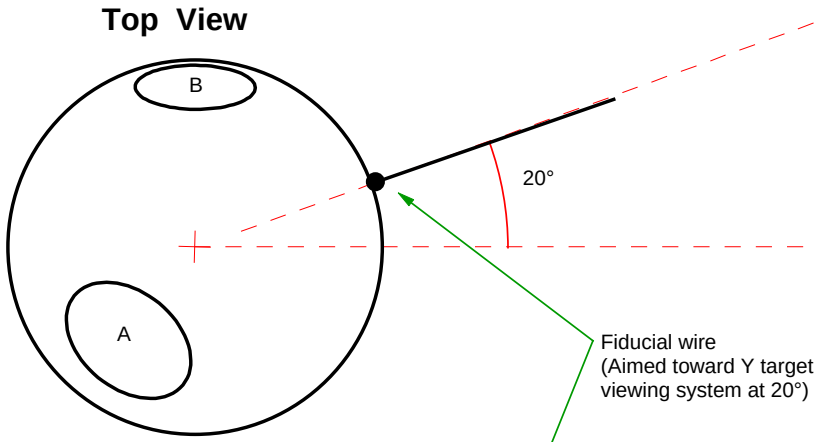

Top View

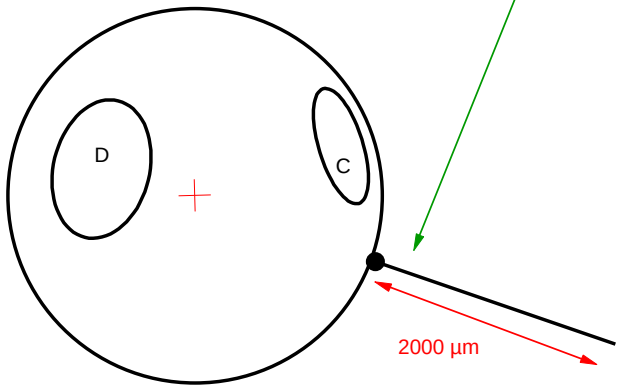

Bottom View

LEH Coordinates:

	Theta	Phi
LEH A:	37.38	234
LEH B:	79.19	90
LEH C:	100.81	342
LEH D:	142.62	198
SOP package	100.81	270
Stalk attachment:	90.00	20
Fidu wire alignment:		20

Tetrahedral Hohlraums for Omega
H4-H7 orientation

Tom Murphy
July 29, 1998

(not drawn to scale)

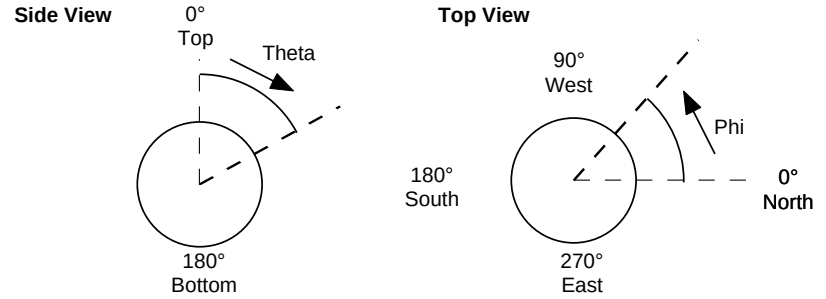

Coordinate System

Thin-wall hohlraums

Inside diameter:	2800 µm
LEH diameter:	700 µm
Gold Thickness:	2 µm
CH Thickness:	100 µm

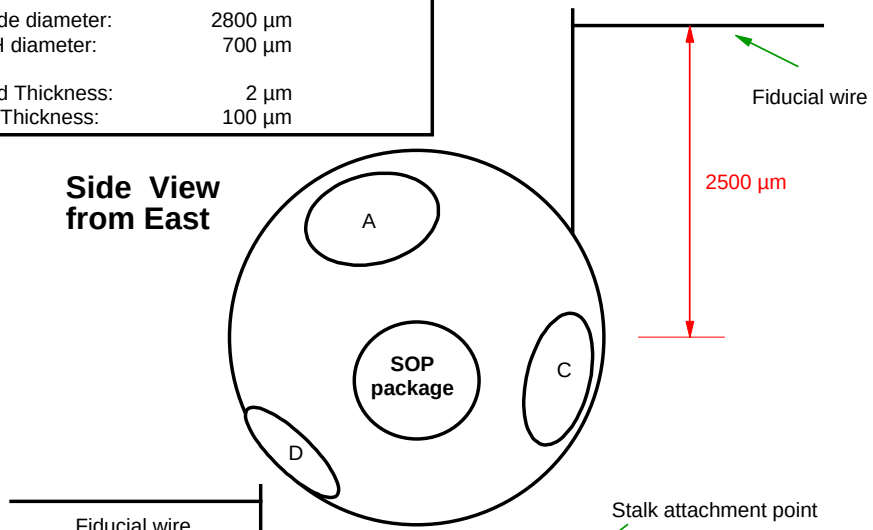

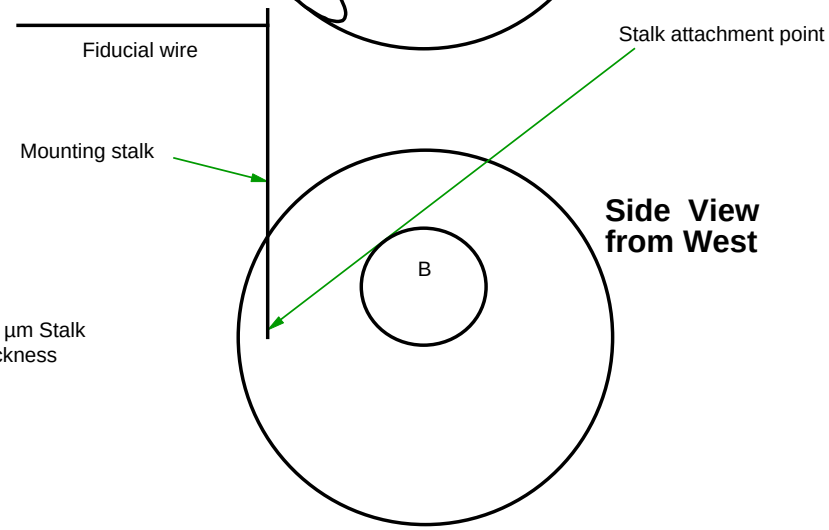

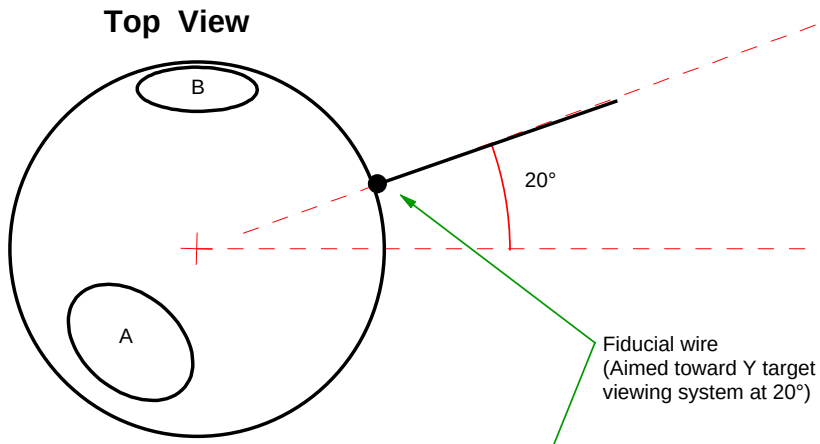

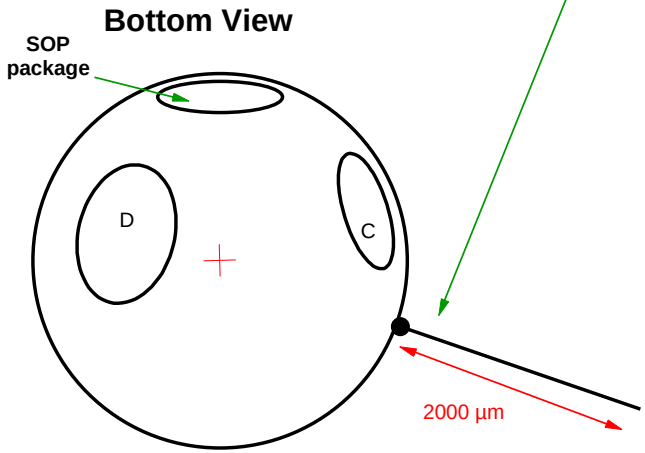

Pre-Shot Report: High Convergence Implosions Within Tetrahedral Hohlraums

09/03/98: Shot Request Forms 4396 - 4409

Guy R. Bennett and Jon H. Wallace (principal investigators)

This note describes the second shot day of Los Alamos' third tetrahedral hohlraum campaign at the Omega laser facility. This three-day series takes place September 2nd - 4th 1998, and consists of three separate experiments of approximately ten shots each:

day #1. Pointing shots, double shells, and drive uniformity (Watt and Kyrala)
day #2. Single shell high convergence implosions (Bennett)
day #3. Indirectly-driven shock wave physics (Kyrala)

This document details all shots fired on the second day. Separate information may be supplied by Watt and Kyrala specifying their goals, etc. It should be noted, however, that all three experiments do require the same tetrahedral illumination and beam pointing; albeit with different pulse shape and energy requirements.

- Require maximum energy using PS22 (340 J/beam) for all 60 beams.

- Tetrahedral hohlraum will be orientated such that the four laser entrance holes (LEH's) align along H4, H7, H13, & H20. Days #1, #2, and #3 will use same hohlraum design and orientation. This affords TIM5 a view of an LEH antinode, and a reasonable dante view into the LEH opposite H20.

Introduction

Although National Ignition Facility (NIF) single shell capsule designs generally specify convergence ratios of $\eta \sim 20 - 35$ [1], the HEP-1 (hydrodynamically equivalent physics campaign #1) Nova experiments, reported in 1994, achieved a more modest convergence ratio maximum of $\eta \sim 24$ [2]. Since the required drive uniformity quality, etc. are rapidly increasing functions of η, it is felt in some circles therefore that this most fundamental of NIF ignition requirements has not been conclusively demonstrated. For the HEP-1 campaign, all ten Nova beams were directed into a uranium cylindrical hohlraum with the same 1:8 (foot to peak) contrast pulse shape (PS26), and the resulting near-planckian x-ray field imploded a very small 132 μm radius capsule filled with deuterium (DD) gas. Measurement of the resulting secondary and primary neutron yields, in conjunction with ion temperature and the secondary neutron spectra (12 - 17 MeV), allowed the nuclear fuel ρr to be determined - from which the convergence ratio was inferred ($\eta = \sqrt{\rho r / \rho_o r_o}$). Within the HEP-1 series, higher convergence ratios were almost certainly limited by the time-dependent x-ray drive asymmetries produced within the cylindrical hohlraums illuminated by a

single laser cone per laser entrance hole (LEH), containing five beams each. Sufficient uniformity has, however, been successfully modeled for the proposed NIF indirect drive scheme; i.e. a total of 192 beams into two LEH's, with independent pulse shapes for the inner and outer rings (96 beams divided unequally into two cones). Indeed, this is the drive configuration around which NIF is presently being constructed. 2D LASNEX simulations of this cylindrical (and therefore two-dimensional) problem, indicate ignition may be extremely sensitive to time-dependent drive non-uniformities - and large yields could become a rather 'hit or miss' affair.

In contrast, the x-ray field generated within a spherical hohlraum with four LEH's placed at the vertices of a tetrahedral, has been experimentally demonstrated by Los Alamos, LLE, and LLNL to be a significant improvement upon the HEP-1 type cylindrical hohlraum drive [3]. Indeed, independent of beam refraction, spot motion, and other physical effects, the tetrahedral drive has spherical-harmonic components $\boldsymbol{l}$ = 1, 2, & 5 which are identically zero [4]. Furthermore, with judiciously chosen beam locations and beam phasing, the $\boldsymbol{l}$ = 4 & 5 contributions can be zeroed at all times (higher order non-zero modes are of lesser importance to field symmetry). Conversely, in cylindrical geometry, one can show only the $m = 0$ even $\boldsymbol{l}$ components may exist; where again lower order modes are most detrimental to implosion symmetry. Complete elimination of the $P_2(\cos\theta)$ and $P_4(\cos\theta)$ requires at least three sets of phased (three cones) beams, although with just two cones per LEH one can achieve $P_2(\cos\theta) = 0$, and a negligible but time-dependent $P_4(\cos\theta)$ asymmetry. This is of course the NIF-like drive configuration, and controlling the $P_4(\cos\theta)$ to acceptable levels is the main cause of the ignition sensitivities which 2D LASNEX calculations have predicted. Interestingly, cylindrical hohlraums have formed the backbone of the US ICF efforts partly because they are two-dimensional, and can therefore be studied and understood using LASNEX; a 2D radiation-hydrodynamics code with the most sophisticated and reliable indirect-drive radiation transport currently available.

The study of NIF-like high convergence implosions within tetrahedral hohlraums during September 3rd, and throughout FY99 (approximately 55 shots in total), can be regarded as an extension to the Nova HEP-1 campaign but with significantly improved x-ray drive symmetry. If very high convergences ($\eta > 30$) are obtained during this long series, the problem of time-dependent drive asymmetry within cylindrical hohlraums could take on renewed interest for NIF. This initial 12 shot experiment will build upon the previous implosion work of the second tetrahedral campaign, performed during August 1997. And will study DD gas fill pressures of 50, 25 and 8 atm, with and without 0.1 atm of Ar doping for x-ray imaging purposes. Although, the August 1997 campaign strongly indicated a much improved x-ray drive, one should not presume tetrahedral hohlraums are problem-free. For instance, to properly illuminate the spherical hohlraum, it is necessary at Omega for all 60 beams to have their focal points located within the radiation case. Blow off plasma from the wall and/or the capsule is then free to interact with the high intensity focal region, with the possibility that hot electrons are generated. The resulting preheat could preclude high convergence. However, preheat problems have not been conclusively observed, although we will be vigorously investigating this in the forthcoming shots; both September 3rd and throughout FY99. Ge doped plastic capsules and uranium tetrahedral hohlraums, used in FY99, may reduce any preheat effects.

High Convergence Targets

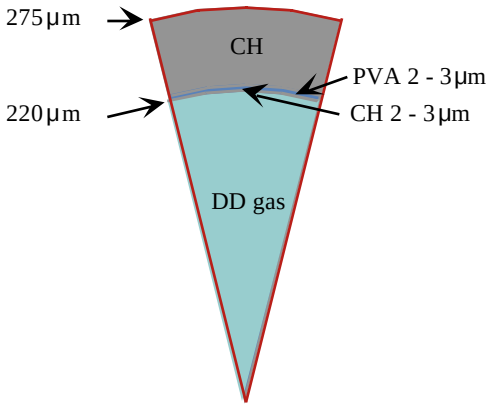

Fig.1. Capsule design to be used for all September 3rd shots. It is the so-called Nova standard capsule. DD gas pressure will range over 50, 25, & 8 atm; with and without 0.1 atm of argon doping for x-ray imaging purposes. These capsules have not been optimized for most NIF-like conditions, but rather build upon Los Alamos' August 1997 campaign. For FY99 (~ 45 high convergence shots), however, the capsules will have minimal preheat, etc. and will produce primary yields hopefully within the optimum operating range of medusa.

All high convergence capsules will be centered within 2800 µm inside diameter gold tetrahedral hohlraums. The four LEH's will be 700 µm in diameter - aligned opposite H4, H7, H13, and H20 - and approximately 100 µm of polystyrene (CH) will support the 2 µm wall thickness. The shot sequence is shown below in table 1.

Wednesday 09/02/98	Thursday 09/03/98	Friday 09/04/98
#1	#1 high con 25 atm with Ar (RID 4396)	#1
#2	#2 high con 8 atm with Ar (RID 4397)	#2
#3	#3 high con 8 atm with Ar (RID 4398)	#3
#4	#4 high con 25 atm with Ar (RID 4399)	#4
#5	#5 high con 25 atm no Ar (RID 4400)	#5
#6	#6 high con 25 atm no Ar (RID 4401)	#6
#7	#7 high con 8 atm no Ar (RID 4402)	*#7*
#8	#8 high con 8 atm no Ar (RID 4403)	*#8*
#9	#9 high con 8 atm no Ar (RID 4404)	*#9*
#10	#10 high con 25 atm no Ar (RID 4405)	*#10*
#11	*#11 high con 25 atm no Ar (RID 4406)*	
#12	*#12 high con 8 atm no Ar (RID 4407)*	
#13	*#13 high con 50 atm no Ar (RID 4408)*	
#14	*#14 high con 50 atm no Ar (RID 4409)*	

Table.1 Shot sequence for the high convergence implosions (Bennett and Wallace). Blank spaces are for pointing shots, double shell implosions, and shock wave physics shots (to be specified by Watt & Varnum and Kyrala & Goldman). Italics denote targets for those days where > 10 shots may be fired. Because 09/04/98 is a non-extended shift day, 6 - 8 shots is most likely.

Nuclear Diagnostics (Vladimir Glebov)

To measure convergence ratios η, the medusa neutron time-of-flight (NTOF) system will be employed. Therefore forming the primary diagnostic for these shots. Of possibly more importance is the DD primary neutron yield measurement using the 'scintillator counters.' Since if the secondary neutron production is too low for medusa then at least 'Yoc' (yield observed over clean calculated) can be obtained. The primary yields may be a little low for indium activation (require > 10^8), although this diagnostic will certainly be used anyway. For the anticipated nuclear ρr values of < 20 mg/cm^2, the secondary neutron production will be rather weakly dependent upon ion temperature (expecting ~ 0.9 keV and a little less for the electron temperature). However, we would certainly like to measure this quantity.

The LASNEX calculated primary yields for the September 3rd capsules are ~ 1 - 5 $\times 10^8$ (accurate to a factor of two or so). However, the Omega DD fuel ion temperature instruments cover ~ 1 - 20 $\times 10^6$ for medusa (> 0.05 keV) and 3 - 40 $\times 10^9$ for the scintillator-PMT (> 0.5 keV) device. Therefore, a gap exists for the yield range of interest. Fortunately, Vladimir Glebov will be able to set up a suitable system using a similar microchannel plate PMT and fast quenched scintillator, coupled to a fast digitizer (involves re-arranging fast digitizers, but is not too time consuming or difficult). Apparently, the detector in mind was left by Michael Cable after his two-year visit to LLE. Incidentally, Dr. Glebov has formal plans to close the gap between 3 $\times 10^7$ and 3×10^9 with a set of detectors capable of measuring both yield and ion temperatures over 10^7 - 10^{14} and 1.0 - 20 keV respectively.

Primary neutron diagnostics are:

(1) medusa
(2) scintillator counters (for primary yield)
(3) indium activation (for primary yield)
(4) M. Cable's MCP-PMT (and V. Glebov's fast digitizer) for ion temperature measurement
(5) LLE bangtime detectors
(6) Los Alamos bangtime detector

X-Ray Diagnostics (Frederic Marshall, Gregory Pien, etc.)

KB3, located in H13, looks directly into an LEH. This instrument has four grazing incidence channels plus one pin hole image (10 μm diameter pinhole and 22.6x magnification). Only time-integration onto film is possible. KB images are 20.3x, and all five channels are usually dispersed by a grating. For our experiment, however, this will be removed. Channels 1 & 2 are filtered by 6 mil of Be (the minimum), whereas 3 & 4 have 1.0 mils of Al as additional filtering. One can adjust the spectral filtering by using 0.5 mil increments of Al. The 0.7 degree mirrors are iridium coated, and the estimated spatial resolution is of order 3 - 10 μm (allowing for motional blur of typical directly-driven imploding capsules, time-integrated onto film).

KB1 located in H8 is directly opposite KB3, and therefore looks through an LEH antipode. This device differs in the reduced magnification (13x for KB and pinhole images) and spatial resolution; plus the use of a 5 rather than 10 μm pinhole. This instrument *will* have a diffraction grating.

Omega has four x-ray framing cameras (XRFC's), each capable of capturing 16 frames (four frames per strip, with adjustable interstrip timing). Apparently XRFC4 is the most sensitive camera (Barnes), and so this instrument will be located in TIM2 for an LEH view. 12x magnification (the maximum available) and 5 μm pinholes (provided by Los Alamos, and metrologized by Guy Bennett) will be employed for optimum image quality of the imploding core.

Primary x-ray diagnostics:

(1) KB3 (with diffraction grating removed) located in H13F (LEH view)
(2) XRFC4 located in TIM2 (LEH view)

Secondary x-ray diagnostics:

(1) XRFC2 in TIM4
(2) XRFC1 in TIM1
(3) PHC in TIM3
(4) Fixed 4x pinhole time-integrated cameras located in P12A, H9C, H8C, H3C, H13C, and H12C
(5) KB1 in H8F
(6) GMXI/KB2 in H9F (crystal removed for polychromatic imaging)

Target Metrology (Peter Gobby, etc.)

The DD filled capsules must be kept in dry ice prior to an experiment. The diffusion rate loss of deuterium, at room temperature, is believed to follow an exponential half life model with τ = 24 - 36 hours (independent of fill pressures for 8 - 25 atm). Because of the uncertainty in τ, the targets must be metrologized extremely quickly (a precisely known τ would allow the DD loss to be calculated exactly); i.e. within an hour or less. During this hour, the most important check will be the capsule location within the spherical hohlraum. Movement of the capsule during travel to Rochester is a possibility, since the formvar web is rather delicate. Thus, the capsule location will be metrologized and compared with pre-travel measurements. Secondly, the rotational alignment fiducial position will be checked and compared with the pre-travel figures. The position of the LEH's with respect to each other and the vertices of a tetrahedral will not of course change; these measurements will be obtained prior to boosting the capsules with DD. On Wednesday August 26th, the targets will be transported to Rochester as carry-on luggage (American Airlines allow 2 kg of dry ice in a vented container); and Mark Bonino will meet Guy Bennett at LLE to transfer the targets into a larger dry ice container until they are needed.

References

[1] J. Lindl, "Development of the indirect-drive approach to inertial confinement fusion and the target physics basis for ignition and gain," Phys. Plasmas **2,** 3933-4024 (1995).
[2] M. D. Cable et al., "Indirectly driven, high convergence inertial confinement fusion implosions," Phys. Rev. Lett. **73**, 2316 (1994).
[3] LANL/LLE tetrahedral campaigns of March and August 1997.
[4] D. W. Phillion and S. M. Pollaine, "Dynamical compensation of irradiation non-uniformities in a spherical hohlraum illuminated with tetrahedral symmetry by laser beams," Phys. Plasmas **1**, 2963 (1994). J. D. Schnittman and R. S. Craxton, "Indirect-drive radiation uniformity in tetrahedral hohlraums," Phys. Plasmas **3**, 3786 (1996).

Appendix A. Nuclear Diagnostic Summary. All Instruments Listed Are Essential!

instrument	purpose	point of contact
medusa	secondary yield and spectra	Vladimir Glebov
scintillator counters	primary yield	Vladimir Glebov
indium activation	primary yield	Vladimir Glebov
Mike Cable's MCP-PMT	ion temperature	Vladimir Glebov
LLE bangtime		Vladimir Glebov
Los Alamos bangtime		T. J. Murphy (LANL)

Appendix B. X-ray Diagnostic Summary

instrument	location	purpose	priority
KB3 (no grating)	H13F (LEH view)	20.3x 4-spec-chan (time integ)	primary
XRFC4 (min filtering)	TIM2 (LEH view)	12x mag imaging (framing)	primary
XRFC2	TIM4	12x mag imaging (framing)	secondary
XRFC1	TIM1	2x mag imaging (framing)	secondary
TIM PHC	TIM3	12x mag imaging (time integ)	secondary
PH1	P12A	4x mag imaging (time integ)	secondary
PH2	H9C	4x mag imaging (time integ)	secondary
PH3	H8C	4x mag imaging (time integ)	secondary
PH4	H3C	4x mag imaging (time integ)	secondary
PH5	H13C (LEH view)	4x mag imaging (time integ)	secondary
PH6	H12C	4x mag imaging (time integ)	secondary
KB1 (with grating)	H8F	13x mag imaging (time integ)	secondary
GMXI/KB2	H9F	13x mag imaging (framing)	secondary

Appendix C. Implosions Studied During First Two Tetrahedral Campaigns

24th - 28th March 1997, six 50 atm implosions were studied (T. J. Murphy). All contained 0.1 atm of argon, and were identical to the capsule shown in figure 1. The first 2 capsules were imploded within scale 1 tetrahedral hohlraums using 1 nsec square, and the middle two used pulse shape PS22 (also scale 1 hohlraums; i.e. 2300 μm inside diameter, and 450 μm LEH radius). The remainder used scale 1.2 hohlraums (2800 μm inside diameter, and 350 μm LEH radius) and 1 nsec square. In firing order, the shot numbers were: 9018, 9021, 9029, 9031, 9050, and 9051.

20th - 22nd August 1997, a total of two 50 atm implosions were studied (N. D. Delamater). Both contained 0.1 atm of argon, and again were identical to the capsule shown in figure 1. The capsules were imploded within scale 1.2 tetrahedral hohlraums using pulse shape PS22. The shots of interest were 10354 and 10355.

Therefore, the only two shots of interest for the high convergence implosions of 09/03/98, are 10354 and 10355; which were both fired on 08/22/97. At this time the medusa diagnostic was not operational, and so the convergence ratios were not measured. However, the primary yields were. Indeed, shot 10354 returned a yield which was 50 - 100 % of the clean 1D LASNEX calculated value. In contrast, the yield of 10355 was much less than anticipated; and this was attributed to the high likelihood that DD gas had diffused through the plastic wall.

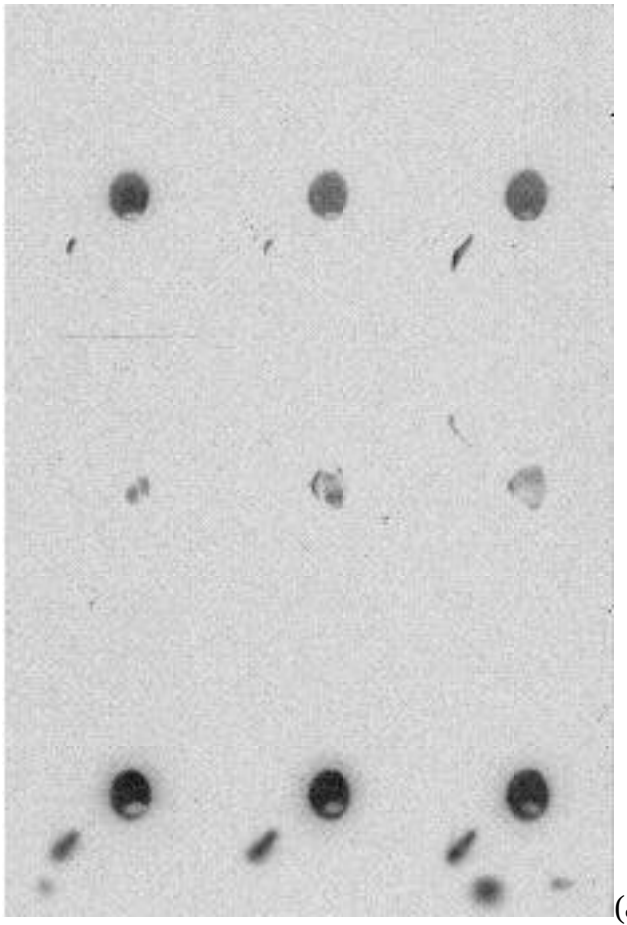
(a)

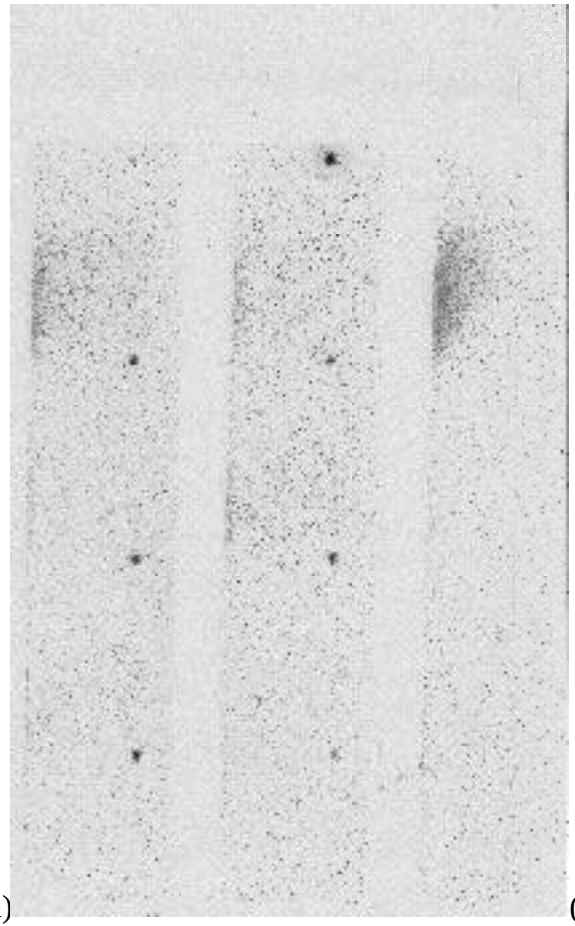
(b)

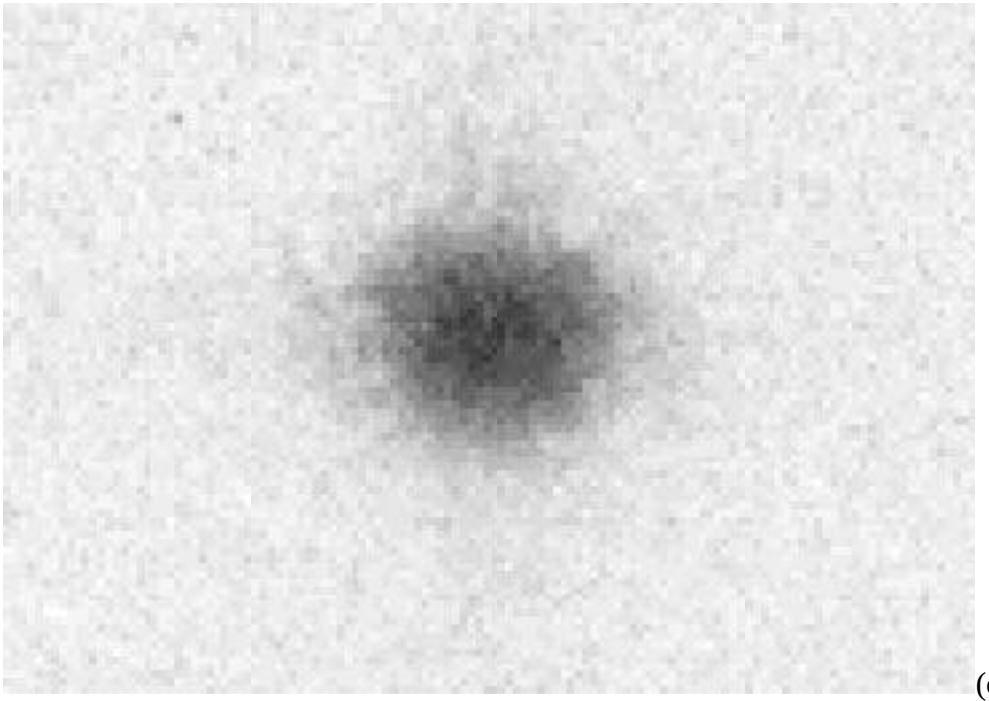

(c)

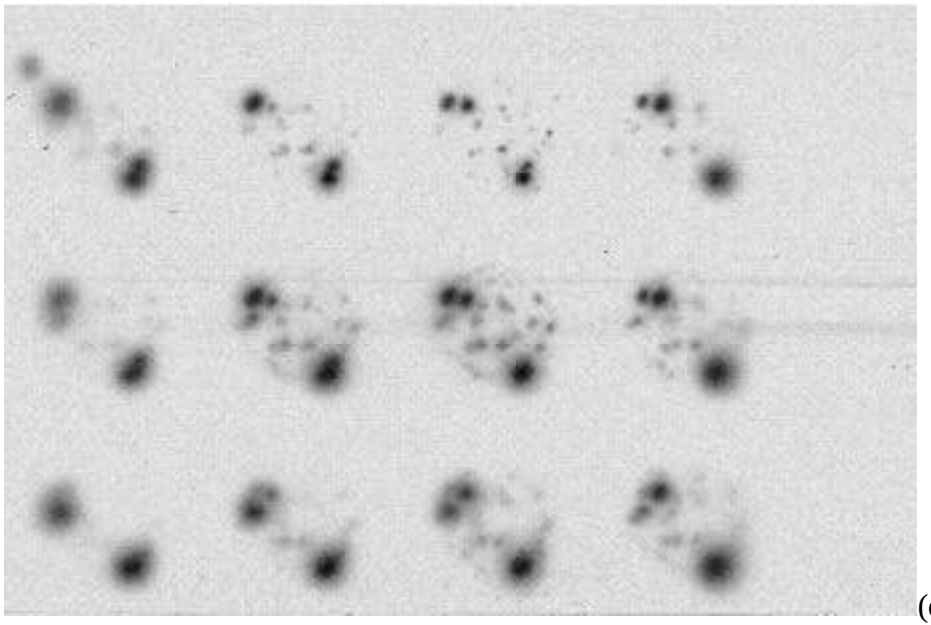

(d)

Fig.2. (a) XRFC1 view through an LEH at a 50 atm DD capsule implosion: shot 10354. Note the capsule is not centered within the spherical hohlraum. (b) Same shot, but XRFC4 view through hohlraum wall at a later time. Both cameras were ran at 12x with 5 μm pinholes. (c) Magnified view of implosion 10355, through an LEH, with the GMXI instrument. (d) 2x framing camera (XRFC2 with 10 μm pinholes) images of the laser spots for shot 10354. Note the film was not flush with MCP, and so the images appears to be out of focus towards the lower strip.

Appendix D. Special Issues For X-Ray Diagnostics

- There are two LEH views: TIM2 and H13. KB3 microscope, located in H13F, will have its grating removed. Use no filtering on channels 1 & 2, but use 1.0 mil Al across 3 & 4. Leave pinhole unfiltered.

- XRFC4 in TIM2 with 10 mil Be filter and 5 micron Los Alamos pinholes (metrologized by Guy Bennett). Set for 12x magnification (essential to use correct 12x alignment pointer). Replace pinholes after each shot, but do not upset nose cone position. Film must always make precise contact with MCP. TIM2 alignment must never change from one shot to another. Set timing as To + 2.2 nsec and 400 psec interstrip delay. Gain = 300. SXRFC (i.e. XRFC3 with LLNL nose cone, located in TIM3) and dante may be used (contact Tom J. Murphy).

- XRFC1 in TIM1 with 10 mil Be filter and 10 micron Los Alamos pinholes. Set for 2x magnification (essential to use correct 2x alignment pointer). Replace pinholes after each shot, but do not upset nose cone position. Film must always make precise contact with MCP. TIM1 alignment must never change from one shot to another. Set timing as To - 0.5 nsec and 400 psec interstrip delay. Gain = 200.

- XRFC2 in TIM4 with 10 mil Be filter and 5 micron Los Alamos pinholes (metrologized by Guy Bennett). Set for 12x magnification (essential to use correct 12x alignment pointer). Replace pinholes after each shot, but do not upset nose cone position. Film must always make precise contact with MCP. TIM4 alignment must never change from one shot to another. Set timing as To + 2.2 nsec and 400 psec interstrip delay. Gain = 200. XRFC2 has an ~ orthogonal view to XRFC4.

- Interstrip timing is defined here to be the time interval between the 1st and 5th (5th & 9th; 9th & 12th) frames receiving the electrical pulse. Therefore, with ~ 150 psec per strip (~ 75 psec per frame), a 400 psec interstrip timing would result in ~ 1.5 nsec of coverage.

- ‘To’ (tee zero) is defined here to be the instant x-ray light first strikes the MCP photocathode. Therefore, a change in magnification of an XRFC will result in different timing, since the MCP location changes.

- Static 4x pinhole cameras used to have 3 x 10 micron pinhole arrays; whereas now, we believe, only single pinholes are employed. For this experiment, we would prefer to use the triple hole substrates if at all possible?

- GMXI/KB2 will be used in the polychromatic mode (crystal removed). The four frames will be set for To + 2.3 nsec and 3/8 nsec interstrip dead time (time interval between 1st frame ending and 2nd one beginning).

Directions to the Laboratory for Laser Energetics

250 E. River Rd.
Rochester, NY
(716) 275-5101
FAX (716) 275-5960